
Boosting Adversarial Robustness and Generalization with Structural Prior

Zhichao Hou¹ Weizhi Gao¹ Hamid Krim¹ Xiaorui Liu¹

Abstract

This work investigates a novel approach to boost adversarial robustness and generalization by incorporating structural prior into the design of deep learning models. Specifically, our study surprisingly reveals that existing dictionary learning-inspired convolutional neural networks (CNNs) provide a false sense of security against adversarial attacks. To address this, we propose Elastic Dictionary Learning Networks (EDLNs), a novel ResNet architecture that significantly enhances adversarial robustness and generalization. This novel and effective approach is supported by a theoretical robustness analysis using influence functions. Moreover, extensive and reliable experiments demonstrate consistent and significant performance improvement on open robustness leaderboards such as RobustBench, surpassing state-of-the-art baselines. To the best of our knowledge, this is the first work to discover and validate that structural prior can reliably enhance deep learning robustness under strong adaptive attacks, unveiling a promising direction for future research.

1. Introduction

In adversarial machine learning, most works have demonstrated their effectiveness in safeguarding deep neural networks by refining the geometry and landscape of parameter space, including robust training (Madry, 2017; Zhang et al., 2019; Gowal et al., 2021) and regularization (Cisse et al., 2017; Zheng et al., 2016). Especially in the visual domain, adversarial training methods powered by generative AI (Wang et al., 2023; Gowal et al., 2021) have achieved remarkable success and dominated the robustness leaderboard (Croce et al., 2020). However, their success increasingly relies on extensive synthetic training data crafted by generative models and increasing networks capacity, pos-

ing critical challenges to breaking through the plateau in adversarial robustness.

In fact, adversarially trained neural networks improve robustness and generalization largely by memorizing adversarial perturbations during training (Madry, 2017). While increasing the backbone model size can enhance memorization capacity, adversarial training methods often suffer from catastrophic *robust overfitting* problem (Rice et al., 2020). Existing methods aim to mitigate robust overfitting from various perspectives, including regularization (Andriushchenko & Flammarion, 2020; Qin et al., 2019; Sriramanan et al., 2020), data augmentation (DeVries, 2017; Zhang, 2017; Carmon et al., 2019; Zhai et al., 2019), and generative modeling techniques (Wang et al., 2023; Gowal et al., 2021). However, all these methods incrementally contribute along a similar trajectory by refining the training strategy, making it difficult to achieve further groundbreaking advancements with the same network capacity.

In this work, we propose to explore an orthogonal direction for innovation upon the finding that most state-of-the-art approaches largely ignore the *structural prior* in deep neural networks. Several works (Papayan et al., 2017; Cazenavette et al., 2021; Mahdizadehghadam et al., 2019; Li et al., 2022) have explored building robust architectures based on sparse coding or dictionary learning priors, assuming that a signal can be sparsely represented as a linear superposition of atoms from a convolutional dictionary. This approach enables natural image patterns to be captured by the sparse code while effectively denoising corruptions. However, their effectiveness has only been validated in scenarios involving weak random corruptions and universal perturbations. Its full potential remains unexplored in the pursuit of stronger adversarial robustness and improved generalization.

To fill this research gap, we revisit dictionary learning in deep learning, which uncovers its inability in handling adaptive adversarial attacks, supported by both empirical evidence and theoretical reasoning. To overcome these limitations, we propose a novel elastic dictionary learning (Elastic DL) framework that complements existing adversarial training methods to achieve superior robustness and generalization. Our contributions are as follows:

- We revisit convolutional dictionary learning in deep learning, highlighting its failures under adaptive attacks, and

¹Department of Computer Science, North Carolina State University, Raleigh, USA. Correspondence to: Xiaorui Liu <xliu96@ncsu.edu>.

provide theoretical insights into these limitations.

- We first propose a robust dictionary learning approach via ℓ_1 -reconstruction and highlight its lower natural performance and the challenges in handling adaptive attacks. Furthermore, we introduce a novel Elastic Dictionary Learning (Elastic DL) framework to enable a better trade-off between natural and robust performance.
- We develop an efficient reweighted iterative shrinkage thresholding algorithm (RISTA) to approximate the non-smooth Elastic DL objective with theoretical convergence guarantees. The algorithm can be seamlessly integrated into deep learning models as a replacement for conventional convolutional layers.
- Extensive experiments demonstrate that our proposed Elastic DL framework can significantly improve adversarial robustness and generalization. Notably, our Elastic DL can achieve state-of-the-art performance, significantly outperforming the previous best defense PORT (Sehwag et al., 2021) on leaderboard across various budgets under ℓ_∞ -norm and ℓ_2 -norm attacks.

2. Related Works

Robust overfitting. Overfitting in adversarially trained deep networks has been shown to significantly harm test robustness (Rice et al., 2020). To address the issue of severe robust overfitting, several efforts have been made from various perspectives. For instance, Dropout (Srivastava et al., 2014) is a widely used regularization method that randomly disables units and connections during training to mitigate overfitting. Regularization techniques (Andriushchenko & Flammarion, 2020; Qin et al., 2019; Sriramanan et al., 2020) have also proven effective in preventing overfitting by penalizing the complexity of model parameters. Data augmentation is another common approach for reducing overfitting in deep network training (Schmidt et al., 2018), with methods including Cutout (DeVries, 2017), Mixup (Zhang, 2017), semi-supervised learning techniques (Carmon et al., 2019; Zhai et al., 2019), and generative modeling (Wang et al., 2023; Gowal et al., 2021) being particularly notable. Additionally, early stopping (Rice et al., 2020) has demonstrated great effectiveness in achieving optimal robust performance during adversarial training. However, existing methods have yet to fully realize the potential of structural priors for improving adversarial robustness and generalization.

Dictionary learning prior in deep learning. Dictionary learning has been well-studied and widely applied in signal and image processing (Olshausen & Field, 1996; Wright et al., 2008; Wright & Ma, 2010; Zhao et al., 2011; Yang et al., 2011; Lu et al., 2013; Chen & Wu, 2013; Jiang et al., 2015; Yang et al., 2011), based on the assumption that an input signal can be represented by a few atoms from

a dictionary. Building on this foundation, Papayan et al. (2017); Cazenavette et al. (2021); Mahdizadehghadam et al. (2019); Li et al. (2022) successfully incorporated dictionary learning into deep learning to interpret or replace the "black-box" nature of neural networks. While these methods have demonstrated promising generalization and robustness against random noise and universal attacks (Li et al., 2022; Mahdizadehghadam et al., 2019), their practical benefits for improving robustness under adaptive attacks are yet to be thoroughly investigated.

We leave the related works about general adversarial attacks and defenses in the Appendix C due to the space limit.

3. Revisiting Convolutional Dictionary Learning in Deep Learning

Notations. Let the input signal be denoted as $\xi \in \mathbb{R}^{H \times W}$ and the convolution kernel as $\alpha \in \mathbb{R}^{k \times k}$, where $k = 2k_0 + 1$. The *convolution* of ξ and α is defined as:

$$(\alpha \star \xi)[i, j] = \sum_{p=-k_0}^{k_0} \sum_{q=-k_0}^{k_0} \xi[i+p, j+q] \cdot \alpha[p, q], \quad (1)$$

while the *transposed convolution* of ξ and α is defined as:

$$(\alpha \star \xi)[i, j] = \sum_{p=-k_0}^{k_0} \sum_{q=-k_0}^{k_0} \xi[i-p, j-q] \cdot \alpha[p, q]. \quad (2)$$

Let the C -channel input signal be denoted as $x = \{\xi_1, \dots, \xi_C\} \in \mathbb{R}^{H \times W \times C}$, and D -channel the output signal as $z = \{\eta_1, \dots, \eta_D\} \in \mathbb{R}^{H \times W \times D}$. The convolution operator $\mathcal{A}(\cdot)$ is associated with kernel \mathbf{A} as:

$$\mathcal{A}(x) = \sum_{c=1}^C (\alpha_{1c} \star \xi_c, \dots, \alpha_{Dc} \star \xi_c) \in \mathbb{R}^{H \times W \times D}. \quad (3)$$

The adjoint transposed convolution operator of \mathcal{A} , denoted as \mathcal{A}^* , is defined as:

$$\mathcal{A}^*(z) = \sum_{d=1}^D (\alpha_{d1} \star \eta_d, \dots, \alpha_{dC} \star \eta_d) \in \mathbb{R}^{H \times W \times C}, \quad (4)$$

where the associated kernel \mathbf{A} is:

$$\mathbf{A} = \begin{pmatrix} \alpha_{11} & \alpha_{12} & \alpha_{13} & \cdots & \alpha_{1C} \\ \alpha_{21} & \alpha_{22} & \alpha_{23} & \cdots & \alpha_{2C} \\ \vdots & \vdots & \vdots & \ddots & \vdots \\ \alpha_{D1} & \alpha_{D2} & \alpha_{D3} & \cdots & \alpha_{DC} \end{pmatrix} \in \mathbb{R}^{D \times C \times k \times k}. \quad (5)$$

Here, H , W , C , D , and k represent the height, width, input dimension, output dimension, and kernel size, respectively.

3.1. Vanilla Dictionary Learning

To enhance the interpretability of black-box deep neural networks (DNNs), Pappayan et al. (2017); Cazenavette et al. (2021); Mahdizadehghadam et al. (2019); Li et al. (2022) introduce the structural prior of dictionary learning into the design of neural networks, assuming that the signal \mathbf{x} can be represented by a linear superposition of several atoms $\{\alpha_{dc}\}$ from a convolutional dictionary \mathbf{A} :

$$\mathbf{x} = \mathcal{A}^*(\mathbf{z}) \in \mathbb{R}^{H \times W \times C}. \quad (6)$$

Then a sparse code \mathbf{z} is sought to extract few descriptors out of the collected dictionary for any given input \mathbf{x} :

$$\min_{\mathbf{z}} \|\mathbf{x} - \mathcal{A}^*(\mathbf{z})\|_2^2 + \lambda \|\mathbf{z}\|_1, \quad (7)$$

where λ is the hyperparameter to balance the fidelity and sparsity terms. Although several works (Cazenavette et al., 2021; Mahdizadehghadam et al., 2019; Li et al., 2022) demonstrated promising robustness of this vanilla dictionary learning (Vanilla DL) defined in Eq. (7) against random corruptions and universal adversarial attacks, it remains unclear whether Vanilla DL can withstand stronger adaptive attacks.

3.2. Preliminary Study: Vanilla DL-based SDNets Is Not Truly Robust

To validate the robustness of Vanilla DL, we conduct a preliminary experiment on SDNet18 (Li et al., 2022), a variant of ResNet18 in which all convolutional layers are replaced with convolutional sparse coding (CSC) layers based on Vanilla DL in Eq. (7). We evaluate the SDNet18 (with fixed λ and tuned λ) under both random impulse noise and adaptive PGD adversarial attack (Madry, 2017) with budget $\frac{8}{255}$. As shown in Table 1, SDNet18 improves upon ResNet18 in terms of robustness against random noise, with more significant improvement achieved by tuning the sparsity weight λ . However, SDNet18 still experiences a sharp drop in performance under adaptive PGD attack, with accuracy approaching zero. The detailed results of the performance under various noise levels and λ values are presented in Figure 11 in Appendix D.1.

Table 1. Preliminary study on SDNet18 (Li et al., 2022) under varying levels of random noise and PGD attack ($\epsilon = \frac{8}{255}$).

MODEL \ NOISE LEVEL	L-1	L-2	L-3	L-4	L-5	PGD
RESNET18	81.44	57.23	48.32	32.49	16.98	0.00
SDNET18 ($\lambda = 0.1$)	82.39	68.90	59.28	40.8	23.83	0.01
SDNET18 (TUNE λ)	82.39	68.90	59.28	43.71	33.43	0.13

In fact, the ℓ_2 -reconstruction term of Vanilla DL in Eq. (7) imposes a quadratic penalty $\|\cdot\|_2^2$ on the residual $\mathbf{x} - \mathcal{A}^*(\mathbf{z})$, making it highly sensitive to outliers introduced by high-level noise and adaptive attacks. The experimental results

reveal that existing Vanilla DL gives a *false sense of security* under random noise and can easily be compromised by adaptive attack. Thus, there still remains a huge gap to achieve truly robust dictionary learning in deep learning.

4. Elastic Dictionary Learning

To overcome the aforementioned limitation brought by the Vanilla DL models, we first propose a robust dictionary learning (Robust DL) via ℓ_1 -reconstruction to mitigate the impact of outlying values in Section 4.1. Moreover, we conduct a comprehensive experiment to demonstrate the advantages of Robust DL and highlight its pitfalls in Section 4.2. Furthermore, to achieve a better inherent trade-off between natural and robust performance, we propose a novel elastic dictionary learning (Elastic DL) approach that enhances both natural performance and robustness in Section 4.3, followed by insightful theoretical robustness analyses in Section 4.4. The overview of our Elastic DL networks (EDLNets) can be found in Figure 1.

4.1. Robust Dictionary Learning via ℓ_1 -Reconstruction

As observed in the previous section, ℓ_2 -fidelity assumes light-tailed noise and performs poorly as the noise becomes increasingly heavy-tailed. To address the sensitivity of ℓ_2 -fidelity in Vanilla DL, we first propose a robust dictionary learning approach (Robust DL) with ℓ_1 -reconstruction to effectively mitigate the impact of outliers:

$$\min_{\mathbf{z}} \|\mathbf{x} - \mathcal{A}^*(\mathbf{z})\|_1 + \lambda \|\mathbf{z}\|_1. \quad (8)$$

Despite the sophisticated design of the model architecture, the ℓ_1 -norm terms in Eq.(8) introduce non-smoothness to the objective function, making it challenging to design an effective and efficient algorithm for approximating the solution. To address this, we first propose a *localized upper bound* as an alternative objective for the ℓ_1 -fidelity term $\|\mathbf{x} - \mathcal{A}^*(\mathbf{z})\|_1$. Subsequently, we employ the iterative shrinkage-thresholding algorithm (ISTA) to solve the ℓ_1 -sparsity.

Localized upper bound. To address $\|\mathbf{x} - \mathcal{A}^*(\mathbf{z})\|_1$ term, we first propose a convex upper bound $\mathcal{U}(\mathbf{z}, \mathbf{z}_*)$ as an alternative in the following Lemma 4.1.

Lemma 4.1. Let $\mathcal{R}(\mathbf{z}) := \|\mathbf{x} - \mathcal{A}^*(\mathbf{z})\|_1$, and for any fixed point \mathbf{z}_* , $\mathcal{U}(\mathbf{z}, \mathbf{z}_*)$ is defined as

$$\mathcal{U}(\mathbf{z}, \mathbf{z}_*) = \|\mathbf{w}^{1/2} \odot (\mathbf{x} - \mathcal{A}^*(\mathbf{z}))\|_2^2 + \mathcal{R}(\mathbf{z}_*), \quad (9)$$

where $\mathbf{w} = \frac{1}{2|\mathbf{x} - \mathcal{A}^*(\mathbf{z}_*)|}$. Then, for any \mathbf{z} , the following holds:

$$(1) \mathcal{U}(\mathbf{z}, \mathbf{z}_*) \geq \mathcal{R}(\mathbf{z}), \quad (2) \mathcal{U}(\mathbf{z}_*, \mathbf{z}_*) = \mathcal{R}(\mathbf{z}_*).$$

Proof. Please refer to Appendix B.1. \square

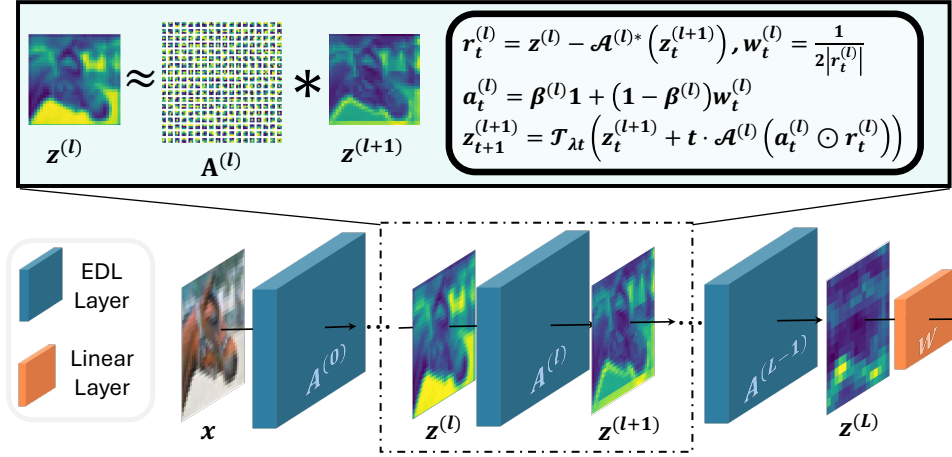


Figure 1. Overview of Elastic DL Networks (EDLNs). EDLNs are constructed by replacing the convolutional layers in conventional backbones (e.g., ResNets) with EDL layers that are unrolled with the proposed efficient RISTA algorithm. Each EDL layer introduces a dictionary structural prior, assuming the input signal $z^{(l)}$ is encoded as a sparse code $z^{(l+1)}$ using a few atoms from diction $A^{(l)}$.

The statement (1) indicates that $\mathcal{U}(z, z_*)$ serves as an upper bound for $\mathcal{R}(z)$, while statement (2) demonstrates that $\mathcal{U}(z, z_*)$ equals $\mathcal{R}(z)$ at point z_* . With fixed z_* , the alternative objective $\mathcal{U}(z, z_*)$ in Eq. (9) is quadratic and can be efficiently optimized. Therefore, instead of minimizing the non-smooth $\mathcal{R}(z)$ directly, we can alternatively optimize the quadratic upper bound $\mathcal{U}(z, z_t)$ with gradient descent algorithm at iteration t .

RISTA algorithm. According to Lemma 4.1, we can find an alternative objective for Eq. (8) at each step t :

$$z_{t+1} = \arg \min_z \|w_t^{1/2} \odot (x - A^*(z))\|_2^2 + \lambda \|z\|_1, \quad (10)$$

where $w_t = \frac{1}{2|x - A^*(z_t)|} \in \mathbb{R}^{H \times W \times C}$. Specifically, when $w_t = \mathbf{1}$, the problem reduces to the formulation in Eq. (7).

Then, we can optimize the ℓ_1 -regularized problem in Eq. (10) instead of original Eq. (8) by our reweighted iterative shrinkage thresholding algorithm (RISTA):

$$z_{t+1} = \mathcal{T}_{\lambda t}(z_t + t \cdot A(w_t \odot (x - A^*(z_t)))), \quad (11)$$

where $\mathcal{T}_{\lambda t}(z) = \text{sign}(z) (|z - \lambda t|)_+$ represents the soft thresholding operator. The detailed derivation of Eq. (11) is provided in Appendix B.2. As a consequence of Lemma 4.1, we can conclude the iteration $\{z_t\}_{t=0}^T$ obtained by Eq. (11) fulfill the loss descent of $\mathcal{R}(z)$:

$$\mathcal{R}(z_{t+1}) \leq \mathcal{U}(z_{t+1}, z_t) \leq \mathcal{U}(z_t, z_t) = \mathcal{R}(z_t).$$

This implies convergence of Eq. (8) can be achieved by optimizing the localized upper bound Eq. (10).

4.2. Pitfalls in ℓ_1 -based Robust DL

To demonstrate the advantages of Robust DL over Vanilla DL, we evaluate the models under random noise and adap-

Table 2. Vanilla DL vs. Robust DL under random corruption (Impulse noise), PGD- ℓ_∞ and PGD- ℓ_2 with various noise levels. Robust DL demonstrates significant improvement over Vanilla DL in robustness but sacrifices natural performance as a trade-off.

	RANDOM	NATURAL	L-1	L-2	L-3	L-4	L-5
VANILLA DL	93.38	84.95	75.83	67.22	44.01	24.91	
ROBUST DL	83.25	77.71	71.69	64.9	51.02	37.78	
PGD-ℓ_∞	NATURAL	1/255	2/255	3/255	4/255	8/255	
VANILLA DL	93.38	59.33	12.64	1.65	0.33	0.01	
ROBUST DL	83.25	64.16	37.76	18.64	8.10	0.20	
PGD-ℓ_2	NATURAL	0.1	0.2	0.3	0.4	0.6	
VANILLA DL	93.38	63.61	27.86	9.78	3.31	0.10	
ROBUST DL	83.25	69.56	50.17	32.58	20.25	2.79	

tive PGD attacks with attack budgets measured in ℓ_∞ and ℓ_2 norms. From Table 2, we observe that ℓ_1 -based Robust DL has the following pitfalls:

- **Pitfall 1: Limited robustness.** In terms of robustness, Robust DL demonstrates a significant advantage over Vanilla DL under high-level random noise and adaptive adversarial attacks (PGD- ℓ_∞ and PGD- ℓ_2) across various budget levels. However, both methods remain vulnerable to adversarially crafted perturbations, achieving nearly zero accuracy under adaptive attacks with imperceptible budgets (8/255 for PGD- ℓ_∞ and 0.6 for PGD- ℓ_2).
- **Pitfall 2: Natural performance sacrifice.** Despite of certain improvement in robustness, Robust DL sacrifices natural performance by 10.13%. We conjecture that although ℓ_1 -based Robust DL effectively mitigates the impact of outlying values, it also misses important information due to the tradeoff between accuracy and robustness.

4.3. Elastic Dictionary Learning

From previous section, we can see that it is not trivial to design an optimal dictionary learning framework with either

ℓ_2 or ℓ_1 reconstruction alone. To this end, we propose an elastic dictionary learning (Elastic DL) to achieve well-balanced trade-off between natural and robust performance:

$$\min_z \frac{\beta}{2} \|\mathbf{x} - \mathcal{A}^*(z)\|_2^2 + \frac{1-\beta}{2} \|\mathbf{x} - \mathcal{A}^*(z)\|_1 + \lambda \|z\|_1, \quad (12)$$

where β is a layer-wise learnable parameter to adaptively balance the two fidelity terms. Similarly, we can generalize the RISTA algorithm from Robust DL to Elastic DL as in Appendix B.2. The RISTA algorithm for the Elastic DL layer is presented in Algorithm 1, and an overview of the entire EDLNet architecture is shown in Figure 1.

Algorithm 1 RISTA for Elastic DL Layer

Input: input signal \mathbf{x} , kernel \mathbf{A} ,
 Initialize $\mathbf{z}_0 \leftarrow \mathcal{A}(\mathbf{x})$
for $t = 1$ **to** $T - 1$ **do**
 $\mathbf{w}_t \leftarrow \frac{1}{2|\mathbf{x} - \mathcal{A}^*(z_t)|}$
 $\mathbf{r}_t \leftarrow (\beta \mathbf{1} + (1 - \beta)\mathbf{w}_t) \odot (\mathbf{x} - \mathcal{A}^*(z_t))$
 $\mathbf{z}_{t+1} \leftarrow \mathcal{T}_{\lambda t}(\mathbf{z}_t + t \cdot \mathcal{A}(\mathbf{r}_t))$
end for
Output: sparse code \mathbf{z}_T

4.4. Theoretical Robustness Analysis

To gain theoretical insight, we conduct a robustness analysis on vanilla, robust, and our elastic dictionary learning using the influence function (Law, 1986), which measures the sensitivity of an operator to perturbations. For simplicity, we consider a single-step case for our RISTA algorithm ($T = 1$) and focus on the analysis of core part \mathbf{r}_t . We derive their influence functions in Theorem 4.2 to demonstrate their sensitivity against input perturbations, with a proof presented in Appendix B.3.

Theorem 4.2 (Robustness Analysis via Influence Function). *The influence function is defined as the sensitivity of the estimate to a small contamination at Δ :*

$$IF(\Delta; \mathcal{P}, \mathbf{y}) = \lim_{t \rightarrow 0^+} \frac{\mathcal{P}(t\Delta + (1-t)\mathbf{y}) - \mathcal{P}(\mathbf{y})}{t}.$$

Let the reconstruction operator is defined as $\mathcal{E}(\cdot) := (\mathbf{I} - \mathcal{A}^* \circ \mathcal{A})(\cdot)$, then the Vanilla, Robust, and Elastic DL operators are $\mathcal{P}_{\text{vanilla}}(\mathbf{x}) = \mathcal{E}(\mathbf{x})$, $\mathcal{P}_{\text{robust}}(\mathbf{x}) = \mathbf{w} \odot \mathcal{E}(\mathbf{x})$, and $\mathcal{P}_{\text{elastic}}(\mathbf{x}) = (\beta \mathbf{1} + (1 - \beta)\mathbf{w}) \odot \mathcal{E}(\mathbf{x})$, where $\mathbf{w} = \frac{1}{2(|\mathcal{E}(\mathbf{x})| + \epsilon)}$ and ϵ is set to avoid zero residual values. Then, we have:

$$IF(\Delta; \mathcal{P}_{\text{vanilla}}, \mathbf{x}) = \mathcal{E}(\Delta - \mathbf{x}),$$

$$IF(\Delta; \mathcal{P}_{\text{robust}}, \mathbf{x}) = 2\epsilon \mathbf{w}^2 \odot \mathcal{E}(\Delta - \mathbf{x}),$$

$$IF(\Delta; \mathcal{P}_{\text{elastic}}, \mathbf{x}) = (\beta \mathbf{1} + 2(1 - \beta)\epsilon \mathbf{w}^2) \odot \mathcal{E}(\Delta - \mathbf{x}).$$

Proof. Please refer to Appendix B.3. \square

Theorem 4.2 offers several insights into the robustness of different dictionary learning methods:

- For Vanilla DL, the influence function is expressed as $\mathcal{E}(\Delta - \mathbf{x})$, indicating that the sensitivity of Vanilla DL is determined by the difference between the noisy sample Δ and the clean sample \mathbf{x} .
- For Robust DL, the influence function is given by $2\epsilon \mathbf{w}^2 \odot \mathcal{E}(\Delta - \mathbf{x})$. The instances with large residuals $|\mathcal{E}(\mathbf{x})|$ are treated as outliers and downweighted by \mathbf{w} . Moreover, while a small ϵ can significantly reduce overall sensitivity, it may also suppress the impact of input variations, leading to natural performance degradation.
- For Elastic DL, the layerwise parameter β can be learned to balance Vanilla and Robust DL, adaptively achieving a better trade-off between natural and robust performance.

5. Experiment

In this section, we comprehensively evaluate the effectiveness of our proposed EDLNet under various experimental settings. Additionally, we provide several ablation studies to demonstrate the working mechanism of our approach.

5.1. Experimental Setting

Datasets. We conduct the experiments on several datasets including CIFAR10 (Krizhevsky et al., 2009), CIFAR100 (Krizhevsky et al., 2009) and Tiny-ImageNet (Le & Yang, 2015).

Backbone architectures. We select ResNets as the backbones, including ResNet10, ResNet18, ResNet34, and ResNet50 (He et al., 2016). Each of the convolutional layers in ResNets are replaced with our Elastic DL layer, resulting in the corresponding EDLNet. We use ResNet18 as the default backbone if not being specified.

Evaluation methods. We evaluate the performance of the models against various attacks, including FGSM (Goodfellow et al., 2014), PGD (Madry, 2017), C&W (Carlini & Wagner, 2017), AutoAttack (Croce & Hein, 2020), and SparseFool (Modas et al., 2019), covering budget measurements across ℓ_∞ -norm, ℓ_2 -norm, and ℓ_1 -norm. For the PGD attack, we consider both ℓ_∞ -norm and ℓ_2 -norm, denoted as PGD- ℓ_∞ and PGD- ℓ_2 , respectively. SparseFool uses the ℓ_1 -norm. Unless otherwise specified, ℓ_∞ is used as the default measurement.

Baselines. For robust overfitting mitigation, we include the baselines including regularization (ℓ_1 , ℓ_2 regularizations and their combination), Cutout (DeVries, 2017), Mixup (Zhang, 2017), and early stopping (Rice et al., 2020). For adversarial training methods, we compare the baselines including PGD-AT (Madry, 2017), TRADES (Zhang et al., 2019),

MART (Wang et al., 2019), SAT (Huang et al., 2020), AWP (Wu et al., 2020), Consistency (Tack et al., 2022), DYNAT (Liu et al., 2024), PORT (Sehwag et al., 2021), and HAT (Rade & Moosavi-Dezfooli, 2022).

Hyperparameter setting. We train the baselines for 200 epochs with batch size 128, weight decay $2e-5$, momentum 0.9, and an initial learning rate of 0.1 that is divided by 10 at the 100-th and 150-th epoch. For our Elastic DL, we pretrain the Vanilla DL model for 150 epochs and then fine-tune the Elastic DL model for 50 epochs.

5.2. Adversarial Robustness & Generalization

First, we validate the effectiveness of our approach in mitigating overfitting. Next, we conduct a comprehensive evaluation of the robustness of adversarial training methods. Finally, we demonstrate that our approach surpasses the state-of-the-art methods on the leaderboard by incorporating structural priors.

Robust overfitting mitigation. To validate the effectiveness of incorporating structural priors, we compare our method with existing popular baselines in mitigating the *robust overfitting* problem in Table 3 and Figure 2. We leave the training curves of all the methods in Appendix D.2.1 and Appendix D.2.2 due to the space limit. From the results, we can make the following observations:

- From Table 3, we observe that our Elastic DL method not only achieves a significant advantage in both absolute FINAL and BEST performance but also maintains a relatively small gap (DIFF) between them, indicating that incorporating the structural prior effectively guides adversarial training to achieve better robustness and generalization.
- From Figure 2, we observe that during the 100th to 200th epochs, the Vanilla DL model exhibits a severe *robust overfitting* phenomenon. By incorporating our Elastic DL structural prior at the 150th epoch, the test robustness improves substantially, highlighting the promising potential of the Elastic DL structural prior in overcoming the bottleneck of adversarial robustness and generalization.

Adversarial training robustness. To validate the effectiveness of our Elastic DL, we select several existing popular adversarial defenses and report the experimental results of backbone ResNet18 under various attacks in Table 4. From the results we can make the following observations:

- Our HAT + Elastic DL significantly outperforms other methods across various attacks, achieving state-of-the-art performance among all baselines.
- Our Elastic DL is a robust architecture that is orthogonal to existing adversarial training methods and can be combined with them to further improve robustness.

Table 3. Natural and robust performance of PGD-based adversarial training with different methods to mitigate the overfitting. BEST represents the highest test accuracy achieved during training, while FINAL is the average accuracy over the last five epochs. DIFF, the difference between BEST and FINAL, measures the ability to mitigate overfitting. The best performance is highlighted in **bold**, while the second-best is underlined.

METHOD	NATURAL ACC.			ROBUST ACC.		
	FINAL	BEST	DIFF	FINAL	BEST	DIFF
VANILLA	78.98	79.90	0.92	44.90	48.01	3.11
ℓ_1 REG.	64.84	65.71	0.87	40.94	41.97	1.03
ℓ_2 REG.	78.88	79.39	0.51	42.73	48.26	5.53
$\ell_2 + \ell_1$ REG.	66.86	67.62	0.76	42.53	43.33	0.80
CUTOUT	75.11	75.58	0.47	47.12	48.23	1.11
MIXUP	69.64	72.05	2.41	46.10	48.53	2.43
EARLY STOPPING	75.51	75.51	0.00	<u>47.69</u>	47.95	0.26
VANILLA DL	82.59	83.27	0.68	44.03	50.53	6.50
ELASTIC DL (OURS)	83.01	83.27	<u>0.26</u>	54.94	55.66	0.72



Figure 2. Test robust accuracy during the adversarial training. we pretrain the Vanilla DL model for 150 epochs and fine-tune the Elastic DL model starting from 150-th epoch. Our Elastic DL method can achieve the best adversarial robustness.

SOTA performance on leaderboard. Furthermore, we validate whether incorporating our structural prior improves over state-of-the-art methods. To achieve this, we select the top-ranking methods, HAT (Rade & Moosavi-Dezfooli, 2022) and PORT (Sehwag et al., 2021), listed on the RobustBench (Croce et al., 2020) leaderboard under ℓ_∞ -norm and ℓ_2 -norm attacks, using ResNet-18 on the CIFAR-10 dataset. As shown in Table 5 (ℓ_∞ -norm attack) and Table 6 (ℓ_2 -norm attack), Our methods, HAT+Elastic DL and PORT+Elastic DL, consistently achieve superior performance in most cases for both natural and robust performances.

5.3. Ablation Study

Universality across datasets and backbones. To validate the consistent effectiveness of our proposed methods, we conduct comprehensive ablation studies on the different backbones (ResNet10, ResNet18, ResNet34, ResNet50), datasets (CIFAR10, CIFAR100, Tiny-ImageNet). As demonstrated in the Figure 3, Table 8, 9 and 10 in Appendix D.3.1, our

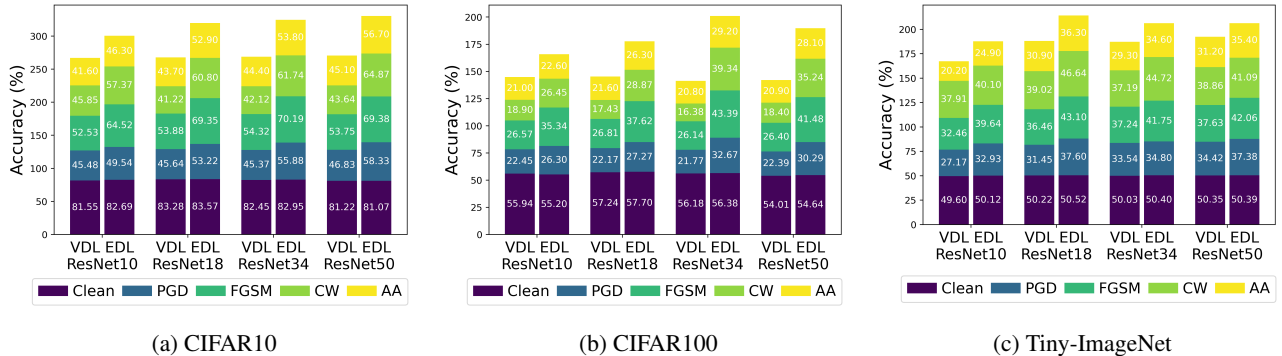


Figure 3. Adversarial robustness under various settings. Our Elastic DL outperforms Vanilla DL across various datasets (CIFAR10 / CIFAR100 / Tiny-ImageNet), backbones (ResNet10 / ResNet18 / ResNet34 / ResNet50) and attacks (PGD / FGSM / CW / AA).

Table 4. Adversarial robustness on CIFAR10 with ResNet18 as backbone. The best performance is highlighted in **bold**.

METHOD	CLEAN	PGD	FGSM	C&W	AA
MART	79.03	48.90	60.86	45.92	43.88
SAT	63.28	43.57	50.13	47.47	39.72
AWP	81.20	51.60	55.30	48.00	46.90
CONSISTENCY	84.37	45.19	53.84	43.75	40.88
DYNAT	82.34	52.25	65.96	52.19	45.10
PGD-AT	80.90	44.35	58.41	46.72	42.14
+ VANILLA DL	83.28	45.64	53.88	41.22	43.70
+ ELASTIC (OURS)	83.57	53.22	69.35	60.80	52.90
TRADES-2.0	82.80	48.32	51.67	40.65	36.40
+ VANILLA DL	79.05	40.64	47.12	41.49	34.90
+ ELASTIC (OURS)	79.85	49.32	58.68	49.47	47.20
TRADES-0.2	85.74	32.63	44.26	26.70	19.00
+ VANILLA DL	82.55	25.37	44.48	30.3	15.30
+ ELASTIC (OURS)	84.75	33.61	57.86	40.68	28.10
PORT	84.59	58.62	62.64	58.12	55.14
+ VANILLA DL	82.35	56.40	60.68	56.77	54.00
+ ELASTIC (OURS)	82.76	59.00	68.54	60.92	56.30
HAT	85.95	56.29	61.17	49.52	53.16
+ VANILLA DL	86.42	57.79	62.67	51.61	54.30
+ ELASTIC (OURS)	86.84	62.48	71.46	59.90	59.07

Table 5. Benchmarking the state-of-the-art performance under ℓ_∞ -norm attack of ResNet18 on CIFAR10.

LEADERBOARD UNDER ℓ_∞ -NORM ATTACK						
BUDGET	CLEAN	PGD- ℓ_∞			AUTOATTACK- ℓ_∞	
	0	8/255	16/255	32/255	8/255	16/255
PORT	84.59	58.62	27.49	5.79	55.14	17.8
+ VANILLA DL	82.35	56.4	27.3	6.38	54.0	20.4
+ ELASTIC (OURS)	82.76	59.0	36.53	22.17	56.3	24.6
HAT	85.95	56.29	25.82	6.09	53.16	17.20
+ VANILLA DL	86.42	57.79	26.08	6.07	54.30	17.56
+ ELASTIC (OURS)	86.84	62.48	44.66	33.69	59.10	29.93

proposed Elastic DL exhibit excellent clean performance and robustness under various attacks.

Orthogonality to adversarial training. Our proposed Elastic DL framework introduce structural prior into neural networks, which is orthogonal with existing adversarial training techniques. As shown in Table 4 and Figure 15 in Appendix D.3.2, our Elastic DL can be combined with different adversarial training (PGD-AT, TRADES-2.0/0.2,

Table 6. Benchmarking the state-of-the-art performance under ℓ_2 -norm attack of ResNet18 on CIFAR10.

LEADERBOARD UNDER ℓ_2 -NORM ATTACK							
BUDGET	CLEAN	PGD- ℓ_2			AUTOATTACK- ℓ_2		
	0	0.5	1.0	2.0	0.5	1.0	2.0
PORT	88.82	74.89	54.47	27.69	73.80	48.1	5.90
+ VANILLA DL	87.34	73.52	53.75	27.5	71.8	49.1	6.7
+ ELASTIC (OURS)	87.81	75.56	60.76	41.44	72.2	52.4	11.1
HAT	89.92	74.68	47.67	21.38	72.9	40.8	2.2
+ VANILLA DL	88.84	67.99	40.87	17.97	66.8	27.8	0.6
+ ELASTIC (OURS)	89.95	74.62	51.41	27.05	73.2	44.5	3.2

PORT, HAT) to further improve the performance.

Different attack measurements. In addition to ℓ_∞ -norm attack (PGD- ℓ_∞), we also validate the consistent effectiveness of our Elastic DL with ℓ_2 -norm (PGD- ℓ_2) and ℓ_1 -norm (SparseFool) attacks in the Figure 16 and Table 11 in Appendix D.3.3.

Hidden embedding visualization. We also conduct visualization analyses on the hidden embedding to obtain better insight into the effectiveness of our proposed Elastic DL. We begin by quantifying the relative difference between clean embeddings (x or z_i) and attacked embeddings (x' or z'_i) across all layers, as shown in Figure 5. Additionally, we visualize one instance in Figure 4, with more examples provided in Appendix D.3.4. The results in Figure 5 show that Elastic DL has smaller embedding difference across layers, indicating that our proposed Elastic DL architecture indeed mitigates the impact of the adversarial perturbation. Moreover, as demonstrated in the example in Figure 4, the presence of adversarial perturbations can disrupt the hidden embedding patterns, leading to incorrect predictions in the case of Vanilla DL. In contrast, our Elastic DL appears to lessen the effects of such perturbations and maintain predicting groundtruth label. From the figures, we can also clearly tell that the difference between clean attacked embeddings of Vanilla DL is much more significant than in Elastic DL.

Convergence. To validate the effectiveness of our RISTA iterations, we plot the loss descent curves of overall ob-

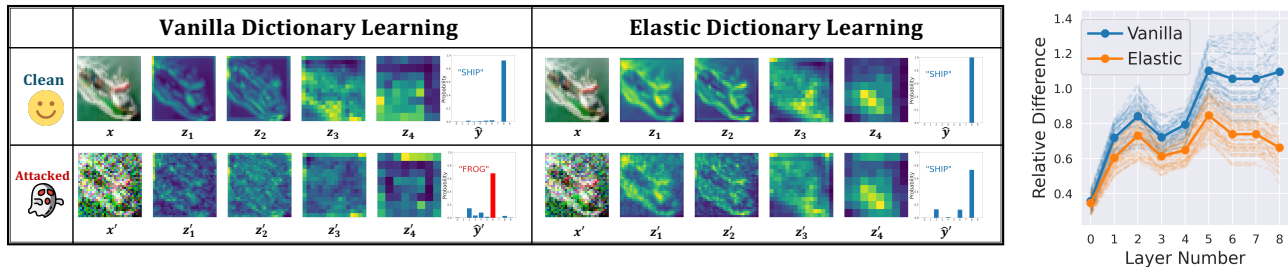


Figure 4. Hidden embedding visualization under clean and attacked scenarios. The difference between clean and attacked embeddings in Elastic DL is smaller compared to Vanilla DL, with this effect becoming more significant in deeper layers. Consequently, while an adversarial attack alters the Vanilla DL output from "SHIP" to "FROG", Elastic DL successfully preserves the correct prediction.

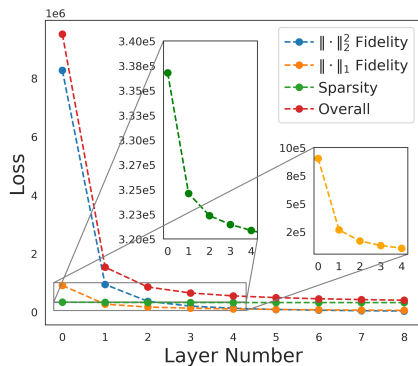


Figure 6. Algorithm convergence. RISTA algorithm achieves fast convergence within just three steps.

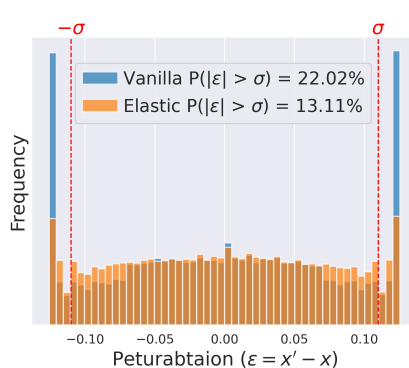


Figure 7. Attack behaviors. The attacker tends to attack Vanilla DL model by introducing outlying values.

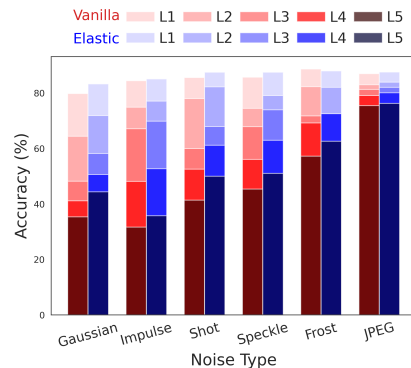


Figure 8. Out-of-distribution robustness. Our Elastic DL also demonstrates excellent out-of-distribution robustness.

jective Eq.(12) along with the individual terms ($\|x - \mathcal{A}^*(z)\|_2^2$, $\|x - \mathcal{A}^*(z)\|_1$ and $\|z\|_1$) in Figure 6, which shows that RISTA converges rapidly within first three steps.

Attack behaviors. To investigate the attack behaviors, we apply the PGD attack to both models and visualize the resulting perturbations in Figure 7. It can be observed that, in the Vanilla DL model, the adversarial attack introduces substantial outlying noise, which can be largely mitigated by our Elastic DL method.

Out-of-distribution Robustness. Beyond in-distribution robustness, we further validate the advantage of our proposed Elastic DL structure by evaluating the out-of-distribution performance of Vanilla DL and Elastic DL. The results in Figure 8 demonstrate the superiority of our Elastic DL over the Vanilla DL under various types of out-of-distribution noise.

Running time analysis. We also perform a analysis to evaluate the inference time of different architectures using ResNet18 as the backbone. We replace multiple convolutional layers in ResNet18 with either Vanilla DL or Elastic DL layers, ranging from 0 to 14 layers. As shown in Table 7, our Elastic DL introduces only a slight computational overhead compared to Vanilla DL and requires 1-3 times

more computation than ResNets, which is considered acceptable. However, our Elastic DL demonstrates significantly improved robustness compared to ResNets and Vanilla DL.

Table 7. Running time (ms) analysis.

LAYERS	0 (RESNET)	2	4	6	8	10	12	14
VANILLA DL	7.82	8.40	9.28	10.51	12.13	13.11	14.16	15.40
ELASTIC DL	7.82	8.90	11.39	13.18	15.99	16.86	19.57	21.94

6. Conclusion

This paper proposes an orthogonal direction to break through the current plateau of adversarial robustness. We begin by revisiting dictionary learning in deep learning and reveal its limitations in dealing with outliers and its vulnerability to adaptive attacks. As a countermeasure, we propose a novel elastic dictionary learning approach along with an efficient RISTA algorithm unrolled as a convolutional neural layers. Our comprehensive experiments demonstrate that our method achieves remarkable robustness, surpassing state-of-the-art baselines available on the robustness leaderboard. To the best of our knowledge, this is the first work to discover and validate that structural prior can reliably enhance adversarial robustness and generalization, unveiling a promising direction for future research.

Impact Statement

Ethical statement. This paper proposes to introduce elastic dictionary learning structural prior to enhance the robustness and safety of machine learning models. We do not identify any potential negative concerns.

Societal consequences. By improving the resilience of machine learning models against adversarial attacks, this research supports the reliable deployment of AI technologies, ensuring their reliability in real-world scenarios and fostering public confidence in their adoption.

References

- Addepalli, S., Jain, S., Sriramanan, G., and Venkatesh Babu, R. Scaling adversarial training to large perturbation bounds. In *European Conference on Computer Vision*, pp. 301–316. Springer, 2022.
- Alzantot, M., Sharma, Y., Chakraborty, S., Zhang, H., Hsieh, C.-J., and Srivastava, M. B. Genattack: Practical black-box attacks with gradient-free optimization. In *Proceedings of the genetic and evolutionary computation conference*, pp. 1111–1119, 2019.
- Andriushchenko, M. and Flammarion, N. Understanding and improving fast adversarial training. *Advances in Neural Information Processing Systems*, 33:16048–16059, 2020.
- Andriushchenko, M., Croce, F., Flammarion, N., and Hein, M. Square attack: a query-efficient black-box adversarial attack via random search. In *European conference on computer vision*, pp. 484–501. Springer, 2020.
- Carlini, N. and Wagner, D. Towards evaluating the robustness of neural networks. In *2017 IEEE Symposium on Security and Privacy (SP)*, pp. 39–57. Ieee, 2017.
- Carmon, Y., Raghuathan, A., Schmidt, L., Duchi, J. C., and Liang, P. S. Unlabeled data improves adversarial robustness. *Advances in neural information processing systems*, 32, 2019.
- Cazenavette, G., Murdock, C., and Lucey, S. Architectural adversarial robustness: The case for deep pursuit. In *Proceedings of the IEEE/CVF Conference on Computer Vision and Pattern Recognition*, pp. 7150–7158, 2021.
- Chen, P.-Y., Zhang, H., Sharma, Y., Yi, J., and Hsieh, C.-J. Zoo: Zeroth order optimization based black-box attacks to deep neural networks without training substitute models. In *Proceedings of the 10th ACM workshop on artificial intelligence and security*, pp. 15–26, 2017.
- Chen, Z. and Wu, Y. Robust dictionary learning by error source decomposition. In *Proceedings of the IEEE International Conference on Computer Vision*, pp. 2216–2223, 2013.
- Cisse, M., Bojanowski, P., Grave, E., Dauphin, Y., and Usunier, N. Parseval networks: Improving robustness to adversarial examples. In *International conference on machine learning*, pp. 854–863. PMLR, 2017.
- Croce, F. and Hein, M. Reliable evaluation of adversarial robustness with an ensemble of diverse parameter-free attacks. In *International conference on machine learning*, pp. 2206–2216. PMLR, 2020.
- Croce, F., Andriushchenko, M., Sehwag, V., DeBenedetti, E., Flammarion, N., Chiang, M., Mittal, P., and Hein, M. Robustbench: a standardized adversarial robustness benchmark. *arXiv preprint arXiv:2010.09670*, 2020.
- DeVries, T. Improved regularization of convolutional neural networks with cutout. *arXiv preprint arXiv:1708.04552*, 2017.
- Feinman, R., Curtin, R. R., Shintre, S., and Gardner, A. B. Detecting adversarial samples from artifacts. *arXiv preprint arXiv:1703.00410*, 2017.
- Goodfellow, I. J., Shlens, J., and Szegedy, C. Explaining and harnessing adversarial examples. *arXiv preprint arXiv:1412.6572*, 2014.
- Gowal, S., Rebuffi, S.-A., Wiles, O., Stimberg, F., Calian, D. A., and Mann, T. A. Improving robustness using generated data. *Advances in Neural Information Processing Systems*, 34:4218–4233, 2021.
- Grosse, K., Manoharan, P., Papernot, N., Backes, M., and McDaniel, P. On the (statistical) detection of adversarial examples. *arXiv preprint arXiv:1702.06280*, 2017.
- Han, X., Ren, T., Nguyen, T., Nguyen, K., Ghosh, J., and Ho, N. Designing robust transformers using robust kernel density estimation. *Advances in Neural Information Processing Systems*, 36, 2024.
- He, K., Zhang, X., Ren, S., and Sun, J. Deep residual learning for image recognition. In *Proceedings of the IEEE conference on computer vision and pattern recognition*, pp. 770–778, 2016.
- Ho, C.-H. and Vasconcelos, N. Disco: Adversarial defense with local implicit functions. *Advances in Neural Information Processing Systems*, 35:23818–23837, 2022.
- Hou, Z., Feng, R., Derr, T., and Liu, X. Robust graph neural networks via unbiased aggregation, 2024a. URL <https://arxiv.org/abs/2311.14934>.

- Hou, Z., Gao, W., Shen, Y., Wang, F., and Liu, X. Pro-transformer: Robustify transformers via plug-and-play paradigm, 2024b. URL <https://arxiv.org/abs/2410.23182>.
- Hou, Z., Torkamani, M., Krim, H., and Liu, X. Robustness reprogramming for representation learning. *arXiv preprint arXiv:2410.04577*, 2024c.
- Huang, L., Zhang, C., and Zhang, H. Self-adaptive training: beyond empirical risk minimization. *Advances in neural information processing systems*, 33:19365–19376, 2020.
- Jiang, W., Nie, F., and Huang, H. Robust dictionary learning with capped l1-norm. In *Twenty-fourth international joint conference on artificial intelligence*, 2015.
- Krizhevsky, A., Hinton, G., et al. Learning multiple layers of features from tiny images. 2009.
- Langley, P. Crafting papers on machine learning. In Langley, P. (ed.), *Proceedings of the 17th International Conference on Machine Learning (ICML 2000)*, pp. 1207–1216, Stanford, CA, 2000. Morgan Kaufmann.
- Law, J. Robust statistics—the approach based on influence functions, 1986.
- Le, Y. and Yang, X. Tiny imagenet visual recognition challenge. *CS 231N*, 7(7):3, 2015.
- Li, B. and Liu, W. Wat: improve the worst-class robustness in adversarial training. In *Proceedings of the AAAI conference on artificial intelligence*, volume 37, pp. 14982–14990, 2023.
- Li, M., Zhai, P., Tong, S., Gao, X., Huang, S.-L., Zhu, Z., You, C., Ma, Y., et al. Revisiting sparse convolutional model for visual recognition. *Advances in Neural Information Processing Systems*, 35:10492–10504, 2022.
- Liu, Z., Duan, H., Liang, H., Long, Y., Snasel, V., Nicosia, G., Ranjan, R., and Ojha, V. Dynamic label adversarial training for deep learning robustness against adversarial attacks. *arXiv preprint arXiv:2408.13102*, 2024.
- Lu, C., Shi, J., and Jia, J. Online robust dictionary learning. In *Proceedings of the IEEE conference on computer vision and pattern recognition*, pp. 415–422, 2013.
- Madry, A. Towards deep learning models resistant to adversarial attacks. *arXiv preprint arXiv:1706.06083*, 2017.
- Mahdizadehghadam, S., Panahi, A., Krim, H., and Dai, L. Deep dictionary learning: A parametric network approach. *IEEE Transactions on Image Processing*, 28(10): 4790–4802, 2019.
- Metzen, J. H., Genewein, T., Fischer, V., and Bischoff, B. On detecting adversarial perturbations. *arXiv preprint arXiv:1702.04267*, 2017.
- Modas, A., Moosavi-Dezfooli, S.-M., and Frossard, P. Sparsefool: a few pixels make a big difference. In *Proceedings of the IEEE/CVF conference on computer vision and pattern recognition*, pp. 9087–9096, 2019.
- Moosavi-Dezfooli, S.-M., Fawzi, A., and Frossard, P. Deepfool: a simple and accurate method to fool deep neural networks. In *Proceedings of the IEEE conference on computer vision and pattern recognition*, pp. 2574–2582, 2016.
- Nie, W., Guo, B., Huang, Y., Xiao, C., Vahdat, A., and Anandkumar, A. Diffusion models for adversarial purification. *arXiv preprint arXiv:2205.07460*, 2022.
- Olshausen, B. A. and Field, D. J. Emergence of simple-cell receptive field properties by learning a sparse code for natural images. *Nature*, 381(6583):607–609, 1996.
- Papernot, N., McDaniel, P., Goodfellow, I., Jha, S., Celik, Z. B., and Swami, A. Practical black-box attacks against machine learning. In *Proceedings of the 2017 ACM on Asia conference on computer and communications security*, pp. 506–519, 2017.
- Papayan, V., Romano, Y., and Elad, M. Convolutional neural networks analyzed via convolutional sparse coding. *Journal of Machine Learning Research*, 18(83):1–52, 2017.
- Qin, C., Martens, J., Goyal, S., Krishnan, D., Dvijotham, K., Fawzi, A., De, S., Stanforth, R., and Kohli, P. Adversarial robustness through local linearization. *Advances in neural information processing systems*, 32, 2019.
- Rade, R. and Moosavi-Dezfooli, S.-M. Reducing excessive margin to achieve a better accuracy vs. robustness trade-off. In *International Conference on Learning Representations*, 2022.
- Rice, L., Wong, E., and Kolter, Z. Overfitting in adversarially robust deep learning. In *International conference on machine learning*, pp. 8093–8104. PMLR, 2020.
- Schmidt, L., Santurkar, S., Tsipras, D., Talwar, K., and Madry, A. Adversarially robust generalization requires more data. *Advances in neural information processing systems*, 31, 2018.
- Sehwag, V., Mahloujifar, S., Handina, T., Dai, S., Xiang, C., Chiang, M., and Mittal, P. Robust learning meets generative models: Can proxy distributions improve adversarial robustness? *arXiv preprint arXiv:2104.09425*, 2021.

- Shi, C., Holtz, C., and Mishne, G. Online adversarial purification based on self-supervision. *arXiv preprint arXiv:2101.09387*, 2021.
- Sriramanan, G., Addepalli, S., Baburaj, A., et al. Guided adversarial attack for evaluating and enhancing adversarial defenses. *Advances in Neural Information Processing Systems*, 33:20297–20308, 2020.
- Srivastava, N., Hinton, G., Krizhevsky, A., Sutskever, I., and Salakhutdinov, R. Dropout: a simple way to prevent neural networks from overfitting. *The journal of machine learning research*, 15(1):1929–1958, 2014.
- Tack, J., Yu, S., Jeong, J., Kim, M., Hwang, S. J., and Shin, J. Consistency regularization for adversarial robustness. In *Proceedings of the AAAI conference on artificial intelligence*, volume 36, pp. 8414–8422, 2022.
- Wang, Y., Zou, D., Yi, J., Bailey, J., Ma, X., and Gu, Q. Improving adversarial robustness requires revisiting misclassified examples. In *International conference on learning representations*, 2019.
- Wang, Z., Pang, T., Du, C., Lin, M., Liu, W., and Yan, S. Better diffusion models further improve adversarial training. In *International Conference on Machine Learning*, pp. 36246–36263. PMLR, 2023.
- Wright, J. and Ma, Y. Dense error correction via ℓ_1 -minimization. *IEEE Trans. Inf. Theor.*, 56(7):3540–3560, July 2010. ISSN 0018-9448. doi: 10.1109/TIT.2010.2048473. URL <https://doi.org/10.1109/TIT.2010.2048473>.
- Wright, J., Yang, A. Y., Ganesh, A., Sastry, S. S., and Ma, Y. Robust face recognition via sparse representation. *IEEE transactions on pattern analysis and machine intelligence*, 31(2):210–227, 2008.
- Wu, D., Xia, S.-T., and Wang, Y. Adversarial weight perturbation helps robust generalization. *Advances in neural information processing systems*, 33:2958–2969, 2020.
- Yang, M., Zhang, L., Yang, J., and Zhang, D. Robust sparse coding for face recognition. In *CVPR 2011*, pp. 625–632. IEEE, 2011.
- Yoon, J., Hwang, S. J., and Lee, J. Adversarial purification with score-based generative models. In *International Conference on Machine Learning*, pp. 12062–12072. PMLR, 2021.
- Zhai, R., Cai, T., He, D., Dan, C., He, K., Hopcroft, J., and Wang, L. Adversarially robust generalization just requires more unlabeled data. *arXiv preprint arXiv:1906.00555*, 2019.
- Zhang, H. mixup: Beyond empirical risk minimization. *arXiv preprint arXiv:1710.09412*, 2017.
- Zhang, H., Yu, Y., Jiao, J., Xing, E., El Ghaoui, L., and Jordan, M. Theoretically principled trade-off between robustness and accuracy. In *International conference on machine learning*, pp. 7472–7482. PMLR, 2019.
- Zhao, C., Wang, X., and Cham, W.-K. Background subtraction via robust dictionary learning. *EURASIP Journal on Image and Video Processing*, 2011:1–12, 2011.
- Zheng, S., Song, Y., Leung, T., and Goodfellow, I. Improving the robustness of deep neural networks via stability training. In *Proceedings of the IEEE conference on computer vision and pattern recognition*, pp. 4480–4488, 2016.

A. Overview of Elastic Dictionary Learning

Overview of Elastic DL neural networks. Here we plot a figure to show the overall pipeline of incorporating Elastic DL structural prior into adversarial training as in Figure 9.

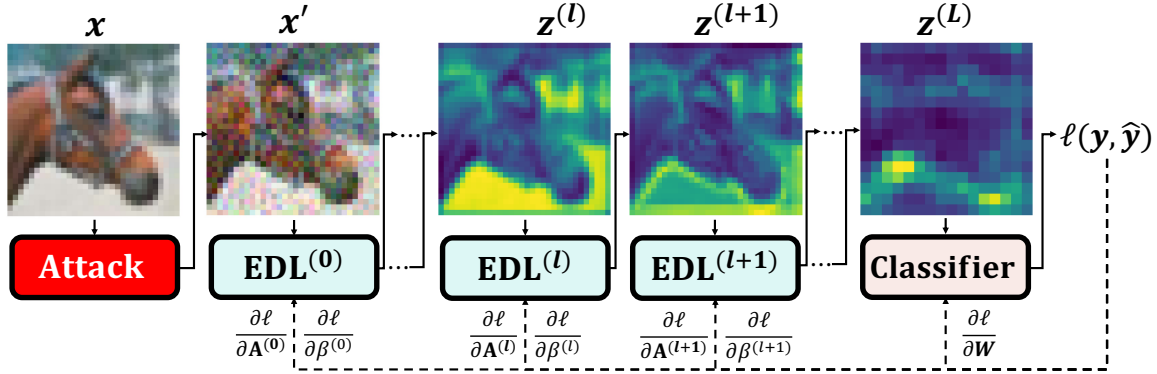


Figure 9. Overview of Elastic DL neural networks in adversarial training. Elastic DL neural networks consist of multiple stacked Elastic DL (EDL) layers. During the forward pass, the input \mathbf{x} is fed into the model, generating a series of hidden codes $\{\mathbf{z}^{(l)}\}_{l=1}^L$ through EDL layers. During the backward pass, the model parameters are updated, including kernel weights $\{\mathbf{A}^{(l)}\}_{l=0}^{L-1}$, layer-wise balance weights $\{\beta^{(l)}\}_{l=0}^{L-1}$, and classifier parameters \mathbf{W} .

Consider a model with $\{\mathbf{A}^{(l)}\}_{l=0}^{L-1}$ and $\{\beta^{(l)}\}_{l=0}^{L-1}$ in the L EDL layers and \mathbf{W} in the classifier. Then, the adversarial training framework with EDL can be formulated as:

$$\begin{aligned} & \min_{\{\mathbf{A}^{(l)}, \beta^{(l)}\}_{l=0}^{L-1}} \mathbb{E}_{(\mathbf{x}, \mathbf{y}) \sim \mathcal{D}} \left[\max_{\mathbf{x}' \in \mathcal{B}(\mathbf{x})} \ell(\mathbf{z}^{*(L)}, \mathbf{y}) \right] \\ \text{s.t. } & \mathbf{z}^{*(l+1)} = \arg \min_{\mathbf{z}} \ell_{NADL}(\mathbf{z}, \mathbf{A}^{(l)}, \mathbf{z}^{*(l)}), \\ & \ell_{NADL}^{(l)}(\mathbf{z}, \mathbf{A}, \mathbf{x}) \text{ is defined in Eq. (12),} \\ & \mathbf{z}^{*(0)} = \mathbf{x}', \\ & \text{for } l = 0, \dots, L-1. \end{aligned}$$

Its overall pipeline can be divided into three main steps as in Figure 9:

- Step 1 (Attack): leverage adversarial attack algorithm (e.g., PGD) to generate worst-case perturbation \mathbf{x}' .
- Step 2 (Forward): input \mathbf{x}' as $\mathbf{z}^{*(0)}$ into model to obtain a series of hidden codes for each layer $\{\mathbf{z}^{(l)}\}_{l=1}^L$ by optimizing dictionary learning loss in Eq. (12).
- Step 3 (Backward): update the model parameters including kernel weights $\{\mathbf{A}^{(l)}\}_{l=0}^{L-1}$, layer-wise balance weight $\{\beta^{(l)}\}_{l=0}^{L-1}$, and other parameters \mathbf{W} .

Exploded view of Elastic DL layer. We also provide an exploded view of each Elastic DL layer as in Figure 10. The input signal $z^{(k)}$ can be represented by a linear superposition of several atoms $\{\alpha_{dc}\}$ from a convolutional dictionary $\mathbf{A}^{(l)}$. Each EDL layer is unrolled using the proposed RISTA algorithm, which approximates the solution for elastic dictionary learning objective.

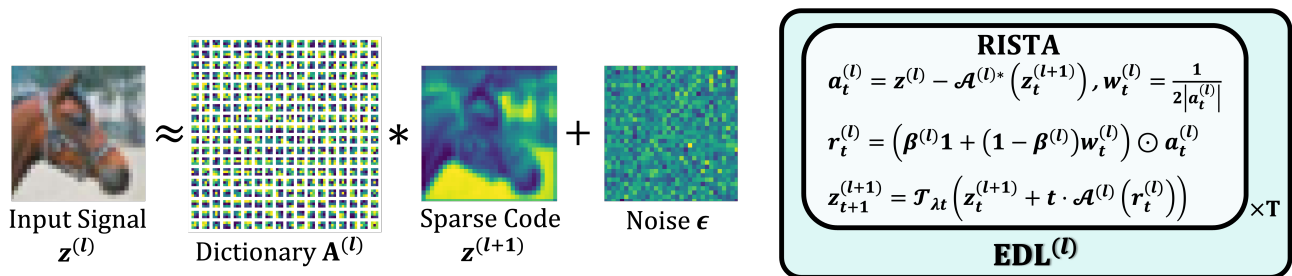


Figure 10. Exploded view of Elastic DL (EDL) layer.

B. Theoretical Proof

B.1. Proof of Lemma 4.1

Proof. Since $\sqrt{a} \leq \frac{a}{2\sqrt{b}} + \frac{\sqrt{b}}{2}$ and the equality holds when $a = b$, by replacemnet as $a = (\mathbf{x}[i, j, c] - \mathcal{A}^*(\mathbf{z})[i, j, c])^2$ and $b = (\mathbf{x}[i, j, c] - \mathcal{A}^*(\mathbf{z}_*)[i, j, c])^2$, then

$$\begin{aligned} |\mathbf{x}[i, j, c] - \mathcal{A}^*(\mathbf{z})[i, j, c]| &\leq \frac{1}{2} \cdot \frac{1}{|\mathbf{x}[i, j, c] - \mathcal{A}^*(\mathbf{z}_*)[i, j, c]|} \cdot (\mathbf{x}[i, j, c] - \mathcal{A}^*(\mathbf{z})[i, j, c])^2 + \frac{1}{2} |\mathbf{x}[i, j, c] - \mathcal{A}^*(\mathbf{z}_*)[i, j, c]| \\ &= \mathbf{w}[i, j, c] \cdot (\mathbf{x}[i, j, c] - \mathcal{A}^*(\mathbf{z})[i, j, c])^2 + \frac{1}{2} |\mathbf{x}[i, j, c] - \mathcal{A}^*(\mathbf{z}_*)[i, j, c]| \end{aligned}$$

Sum up the items on both sides, we obtain

$$\begin{aligned} \mathcal{E}(\mathbf{z}) = \|\mathbf{x} - \mathcal{A}^*(\mathbf{z})\|_1 &= \sum_{i,j,c} |\mathbf{x}[i, j, c] - \mathcal{A}^*(\mathbf{z})[i, j, c]| \\ &\leq \sum_{i,j,c} \mathbf{w}[i, j, c] \cdot (\mathbf{x}[i, j, c] - \mathcal{A}^*(\mathbf{z})[i, j, c])^2 + \frac{1}{2} \sum_{i,j,c} |\mathbf{x}[i, j, c] - \mathcal{A}^*(\mathbf{z}_*)[i, j, c]| \\ &= \|\mathbf{w}^{1/2} \odot (\mathbf{x} - \mathcal{A}^*(\mathbf{z}))\|_2^2 + \mathcal{E}(\mathbf{z}_*) \\ &= \mathcal{U}(\mathbf{z}, \mathbf{z}_*) \end{aligned}$$

and the equality holds at $a = b$ ($\mathbf{z} = \mathbf{z}_*$):

$$\mathcal{U}(\mathbf{z}_*, \mathbf{z}_*) = \mathcal{E}(\mathbf{z}_*). \quad (13)$$

□

B.2. Proof of Algorithm Iteration in Eq. (11)

Here, we derive the algorithm for general elastic dictionary learning (Elastic DL), the ℓ_1 -based robust dictionary learning (Robust DL) can be consider as the special case with $\beta = 0$.

Proof. For convex objective:

$$f(\mathbf{z}) = \frac{\beta}{2} \|\mathbf{x} - \mathcal{A}^*(\mathbf{z})\|_2^2 + \frac{1-\beta}{2} \|(\mathbf{w}^{(t)})^{1/2} \odot (\mathbf{x} - \mathcal{A}^*(\mathbf{z}))\|_2^2,$$

we can achieve the optima via the first-order gradient descent:

$$\mathbf{z}_{t+1} = \mathbf{z}_t - t \nabla f(\mathbf{z}_t),$$

or equivalently,

$$\mathbf{z}_{t+1} = \arg \min_{\mathbf{z}} \{f(\mathbf{z}_t) + \langle \mathbf{z} - \mathbf{z}_t, \nabla f(\mathbf{z}_t) \rangle + \frac{1}{2t} \|\mathbf{z} - \mathbf{z}_t\|^2\}.$$

Then, for the corresponding ℓ_1 -regularized problem:

$$\min_{\mathbf{z}} f(\mathbf{z}) + \lambda \|\mathbf{z}\|_1,$$

we have:

$$\begin{aligned} \mathbf{z}_{t+1} &= \arg \min_{\mathbf{z}} \{f(\mathbf{z}_t) + \langle \mathbf{z} - \mathbf{z}_t, \nabla f(\mathbf{z}_t) \rangle + \frac{1}{2t} \|\mathbf{z} - \mathbf{z}_t\|^2 + \lambda \|\mathbf{z}\|_1\} \\ &= \arg \min_{\mathbf{z}} \left\{ \frac{1}{2t} \|\mathbf{z} - (\mathbf{z}_t - t \nabla f(\mathbf{z}_t))\|^2 + \lambda \|\mathbf{z}\|_1 \right\} \\ &= \arg \min_{\mathbf{z}} \{g(\mathbf{z}) := \frac{1}{2t} \|\mathbf{z} - \mathbf{y}\|^2 + \lambda \|\mathbf{z}\|_1\} \quad (\mathbf{y} = \mathbf{z}_t - t \nabla f(\mathbf{z}_t)) \end{aligned}$$

Then, the optimality condition is:

$$\begin{aligned}
 0 &\in \partial_{\mathbf{z}} g(\mathbf{z}^*) = \frac{1}{t}(\mathbf{z}^* - \mathbf{y}) + \lambda \text{sign}(\mathbf{z}^*) \\
 \Leftrightarrow \mathbf{y} &\in \mathbf{z}^* + \lambda t \text{sign}(\mathbf{z}^*) \\
 \Leftrightarrow \mathbf{y} &\in (\text{Id} + \lambda t \text{sign}(\cdot))(\mathbf{z}^*) \\
 \Leftrightarrow \mathbf{z}^* &= \mathcal{T}_{\lambda t}(\mathbf{y}) := (\text{Id} + \lambda t \text{sign}(\cdot))^{-1}(\mathbf{y}) = \text{sign}(\mathbf{y}) (|\mathbf{y} - \lambda t|)_+.
 \end{aligned}$$

Since

$$\begin{aligned}
 \nabla f(\mathbf{z}) &= -\beta \mathcal{A}(\mathbf{x} - \mathcal{A}^*(\mathbf{z})) - (1 - \beta) \mathcal{A}(\mathbf{w}^{(t)}) \odot (\mathbf{x} - \mathcal{A}^*(\mathbf{z})) \\
 &= -\mathcal{A}\left(\left(\beta \mathbf{1} + (1 - \beta) \mathbf{w}^{(t)}\right) \odot (\mathbf{x} - \mathcal{A}^*(\mathbf{z}))\right),
 \end{aligned}$$

Then

$$\mathbf{z}_{t+1} = \mathbf{z}^* = \mathcal{T}_{\lambda t}(\mathbf{y}) = \mathcal{T}_{\lambda t}(\mathbf{z}_t - t \cdot \nabla f(\mathbf{z})) = \mathcal{T}_{\lambda t}\left(\mathbf{z}_t + t \cdot \mathcal{A}\left(\left(\beta \mathbf{1} + (1 - \beta) \mathbf{w}^{(t)}\right) \odot (\mathbf{x} - \mathcal{A}^*(\mathbf{z}_t))\right)\right)$$

□

B.3. Proof of Theorem 4.2

Proof. Let $\mathbf{x}_t := t\Delta + (1 - t)\mathbf{x}$, $\mathbf{w}_t = \frac{1}{2(|\mathcal{E}(\mathbf{x}_t)| + \epsilon)}$, then

$$\begin{aligned}
 &IF(\Delta; \mathcal{P}_{\text{vanilla}}, \mathbf{x}) \\
 &= \lim_{t \rightarrow 0^+} \frac{\mathcal{P}_{\text{vanilla}}(\mathbf{x}_t) - \mathcal{P}_{\text{vanilla}}(\mathbf{x})}{t} \\
 &= \lim_{t \rightarrow 0^+} \frac{\mathcal{E}(\mathbf{x}_t) - \mathcal{E}(\mathbf{x})}{t} \\
 &= \lim_{t \rightarrow 0^+} \frac{\mathcal{E}(t\Delta + (1 - t)\mathbf{x}) - \mathcal{E}(\mathbf{x})}{t} \\
 &= \mathcal{E}(\Delta - \mathbf{x})
 \end{aligned}$$

Given a small enough t , we can have $\text{sign}(\mathcal{E}(\mathbf{x}_t)) = \text{sign}(\mathcal{E}(\mathbf{x}))$, then

$$\begin{aligned}
 &\mathbf{w}_t - \mathbf{w} \\
 &= \frac{1}{2(|\mathcal{E}(\mathbf{x}_t)| + \epsilon)} - \frac{1}{2(|\mathcal{E}(\mathbf{x})| + \epsilon)} \\
 &= \frac{|\mathcal{E}(\mathbf{x})| - |\mathcal{E}(\mathbf{x}_t)|}{2(|\mathcal{E}(\mathbf{x}_t)| + \epsilon)(|\mathcal{E}(\mathbf{x})| + \epsilon)} \\
 &= -\frac{\text{sign}(\mathcal{E}(\mathbf{x})) \odot (\mathcal{E}(\mathbf{x}_t) - \mathcal{E}(\mathbf{x}))}{2(|\mathcal{E}(\mathbf{x}_t)| + \epsilon)(|\mathcal{E}(\mathbf{x})| + \epsilon)}
 \end{aligned}$$

So

$$\lim_{t \rightarrow 0^+} \frac{\mathbf{w}_t - \mathbf{w}}{t} = \lim_{t \rightarrow 0^+} -\frac{\text{sign}(\mathcal{E}(\mathbf{x})) \odot (\mathcal{E}(\mathbf{x}_t) - \mathcal{E}(\mathbf{x}))}{2t(|\mathcal{E}(\mathbf{x}_t)| + \epsilon)(|\mathcal{E}(\mathbf{x})| + \epsilon)} = -\frac{\text{sign}(\mathcal{E}(\mathbf{x})) \odot (\mathcal{E}(\Delta - \mathbf{x}))}{2(|\mathcal{E}(\mathbf{x})| + \epsilon)^2}$$

Since

$$\begin{aligned}
 &\mathcal{P}_{\text{robust}}(\mathbf{x}_t) - \mathcal{P}_{\text{robust}}(\mathbf{x}) \\
 &= \mathbf{w}_t \odot \mathcal{E}(\mathbf{x}_t) - \mathbf{w} \odot \mathcal{E}(\mathbf{x}) \\
 &= (\mathbf{w}_t - \mathbf{w}) \odot \mathcal{E}(\mathbf{x}) + \mathbf{w} \odot (\mathcal{E}(\mathbf{x}_t) - \mathcal{E}(\mathbf{x})) + (\mathbf{w}_t - \mathbf{w}) \odot (\mathcal{E}(\mathbf{x}_t) - \mathcal{E}(\mathbf{x}))
 \end{aligned}$$

Then we have

$$\begin{aligned}
 & IF(\Delta; \mathcal{P}_{\text{robust}}, \mathbf{x}) \\
 &= \lim_{t \rightarrow 0^+} \frac{\mathcal{P}_{\text{robust}}(\mathbf{x}_t) - \mathcal{P}_{\text{robust}}(\mathbf{x})}{t} \\
 &= \lim_{t \rightarrow 0^+} \frac{\mathbf{w}_t - \mathbf{w}}{t} \odot \mathcal{E}(\mathbf{x}) + \mathbf{w} \odot \lim_{t \rightarrow 0^+} \frac{\mathcal{E}(\mathbf{x}_t) - \mathcal{E}(\mathbf{x})}{t} + 0 \\
 &= -\frac{\text{sign}(\mathcal{E}(\mathbf{x})) \odot \mathcal{E}(\Delta - \mathbf{x})}{2(|\mathcal{E}(\mathbf{x})| + \epsilon)^2} \odot \mathcal{E}(\mathbf{x}) + \mathbf{w} \odot \mathcal{E}(\Delta - \mathbf{x}) \\
 &= -\frac{|\mathcal{E}(\mathbf{x})|}{2(|\mathcal{E}(\mathbf{x})| + \epsilon)^2} \odot \mathcal{E}(\Delta - \mathbf{x}) + \frac{1}{2(|\mathcal{E}(\mathbf{x})| + \epsilon)} \odot \mathcal{E}(\Delta - \mathbf{x}) \\
 &= 2\epsilon \mathbf{w}^2 \odot \mathcal{E}(\Delta - \mathbf{x}),
 \end{aligned}$$

and

$$\begin{aligned}
 & IF(\Delta; \mathcal{P}_{\text{elastic}}, \mathbf{x}) \\
 &= \lim_{t \rightarrow 0^+} \frac{\mathcal{P}_{\text{elastic}}(\mathbf{x}_t) - \mathcal{P}_{\text{elastic}}(\mathbf{x})}{t} \\
 &= \beta IF(\Delta; \mathcal{P}_{\text{vanilla}}, \mathbf{x}) + (1 - \beta) IF(\Delta; \mathcal{P}_{\text{robust}}, \mathbf{x}) \\
 &= (\beta \mathbf{1} + 2(1 - \beta)\epsilon \mathbf{w}^2) \odot \mathcal{E}(\Delta - \mathbf{x}).
 \end{aligned}$$

□

C. Related Works

C.1. Adversarial Attacks

Adversarial attacks are typically classified into two main categories: *white-box* and *black-box* attacks. In white-box attacks, the attacker has full knowledge of the target neural network, including its architecture, parameters, and gradients. Common examples of white-box attacks include gradient-based methods such as FGSM (Goodfellow et al., 2014), DeepFool (Moosavi-Dezfooli et al., 2016), PGD (Madry, 2017), and the C&W attack (Carlini & Wagner, 2017). In contrast, black-box attacks operate under limited information, where the attacker can only interact with the model through its input-output behavior without direct access to internal details. Examples of black-box methods include surrogate model-based approaches (Papernot et al., 2017), zeroth-order optimization techniques (Chen et al., 2017), and query-based methods (Andriushchenko et al., 2020; Alzantot et al., 2019).

Here we list the detailed information of attacks we use in the main paper:

- **Fast Gradient Sign Method (FGSM)** (Goodfellow et al., 2014): FGSM is one of the earliest and most widely used adversarial attack methods. It generates adversarial examples by using the gradient of the loss function with respect to the input data to craft small but purposeful perturbations that lead the model to make incorrect predictions.
- **Projected Gradient Descent (PGD)** (Madry, 2017): PGD is an iterative and more robust extension of FGSM. It repeatedly applies small perturbations within a defined range (or epsilon ball) to maximize the model’s loss. PGD is often considered a strong adversary in the evaluation of model robustness.
- **Carlini & Wagner Attack (C&W)** (Carlini & Wagner, 2017): This attack focuses on crafting adversarial examples by optimizing a custom loss function designed to minimize perturbations while ensuring the generated adversarial samples are misclassified.
- **AutoAttack** (Croce & Hein, 2020): AutoAttack is an ensemble of adversarial attack methods that automatically evaluates the robustness of models. It combines various attacks to provide a strong, reliable benchmark for adversarial robustness without manual tuning.
- **SparseFool** (Modas et al., 2019): SparseFool is a sparse adversarial attack designed to generate adversarial examples by perturbing only a few pixels in the input image. It highlights how minimal changes can significantly alter model predictions.

C.2. Adversarial Defenses

Significant efforts have been devoted to enhancing model robustness through a variety of strategies, including detection techniques (Metzen et al., 2017; Feinman et al., 2017; Grosse et al., 2017; Sehwag et al., 2021; Rade & Moosavi-Dezfooli, 2022; Addepalli et al., 2022), purification-based approaches (Ho & Vasconcelos, 2022; Nie et al., 2022; Shi et al., 2021; Yoon et al., 2021), robust training methods (Madry, 2017; Zhang et al., 2019; Goyal et al., 2021; Li & Liu, 2023), and regularization-based techniques (Cisse et al., 2017; Zheng et al., 2016). Among these, adversarial training-based methods (Sehwag et al., 2021; Rade & Moosavi-Dezfooli, 2022; Addepalli et al., 2022) have proven highly effective against adaptive adversarial attacks, consistently leading the robustness leaderboard (RobustBench) (Croce et al., 2020). Despite their success, most existing methods rely heavily on extensive synthetic training data generated by advanced models, larger network architectures, and empirically driven training strategies. These dependencies pose substantial challenges to advancing beyond the current plateau in adversarial robustness. In this work, we introduce an elastic dictionary framework that incorporates structural priors into model design. This approach is fully orthogonal to existing methods and offers a complementary pathway to further enhance robustness when integrated with current techniques.

Here are we list the detailed information of adversarial training based methods we use in the main paper:

- **PGD-AT** (Madry, 2017): Projected Gradient Descent Adversarial Training (PGD-AT) is a fundamental adversarial training approach that enhances model robustness by iteratively generating adversarial examples using PGD and training the model on them.
- **TRADES** (Zhang et al., 2019): TRADES (Tradeoff-inspired Adversarial Defense via Surrogate Loss Minimization) balances robustness and accuracy by introducing a regularization term that penalizes the discrepancy between natural and adversarial predictions.

- MART (Wang et al., 2019): Misclassification-Aware Adversarial Training (MART) improves robustness by assigning higher weights to misclassified examples, emphasizing correctly classified samples' robustness.
- SAT (Huang et al., 2020): Self-Adaptive Training (SAT) refines adversarial training by adjusting the training process based on the model's confidence, mitigating the effects of incorrect labels and improving generalization.
- AWP (Wu et al., 2020): Adversarial Weight Perturbation (AWP) enhances robustness by perturbing model parameters within a constrained space to improve the worst-case performance against adversarial attacks.
- Consistency (Tack et al., 2022): Consistency training leverages perturbation-invariant representations to enhance robustness by enforcing consistent predictions across different transformations of inputs.
- DYNAT (Liu et al., 2024): Dynamic Adversarial Training (DYNAT) adapts training strategies dynamically based on model performance, balancing robustness and generalization efficiency.
- PORT (Sehwag et al., 2021): Proxy Distribution-based Robust Training (PORT) leverages data from proxy distributions, such as those generated by advanced generative models, to enhance adversarial robustness. By formally analyzing robustness transfer and optimizing training, PORT demonstrates significant improvements in robustness under various threat models.
- HAT (Rade & Moosavi-Dezfooli, 2022): Helper-based Adversarial Training (HAT) mitigates the accuracy-robustness trade-off by incorporating additional incorrectly labeled examples during training. This approach reduces excessive margin changes along certain adversarial directions, improving accuracy without compromising robustness and achieving a better trade-off compared to existing methods.

C.3. Robust Architectures from Robust Statistics Perspective

Several studies have explored constructing robust architectures from the perspective of robust statistics. For instance, RUNG (Hou et al., 2024a) develops robust graph neural networks through unbiased aggregation. Han et al. (2024) design robust transformers using robust kernel density estimation. ProTransformer (Hou et al., 2024b) introduces a novel robust attention mechanism with a robust estimator applied to token embeddings. Additionally, Hou et al. (2024c) propose a universal hybrid architecture inspired by robust statistics, which can be flexibly deployed through robustness reprogramming.

D. Additional Experiments

D.1. Preliminary Studies

Preliminary in SDNet18. We evaluate Vanilla DL (with both fixed and tuned λ) under random impulse noise and adaptive PGD adversarial attacks (Madry, 2017). As illustrated in Figure 11, increasing the noise level and intensifying the distribution tail degradation lead to a decline in Vanilla DL’s accuracy. While tuning the sparsity weight λ enhances resilience to random noise, models with any λ suffer a sharp performance drop under adaptive PGD attacks, with accuracy nearing zero.

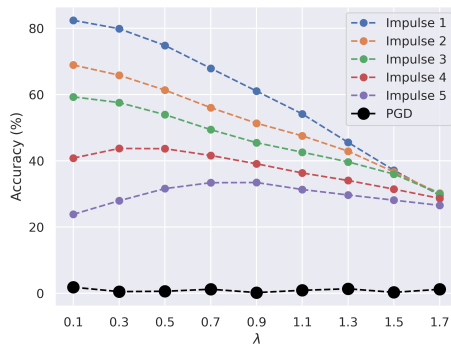


Figure 11. Performance of SDNet18 (Vanilla DL) under random Impulse noise with different levels.

D.2. Adversarial Training Curves

D.2.1. TRAINING CURVES OF EACH METHOD

Training curve of our Elastic DL. From Figure 12, we can observe that during the 100th - 150th epochs, the Vanilla DL model exhibits a severe *robust overfitting* phenomenon: while training performance improves, the test robust accuracy drops significantly. After incorporating our Elastic DL structural prior at the 150th epoch, both training and testing robustness improve substantially. Although there is a slight drop in natural performance during the initial switching period, it recovers quickly within a few epochs. This phenomenon highlights the promising potential of the Elastic DL structural prior in breaking through the bottleneck of adversarial robustness and generalization.

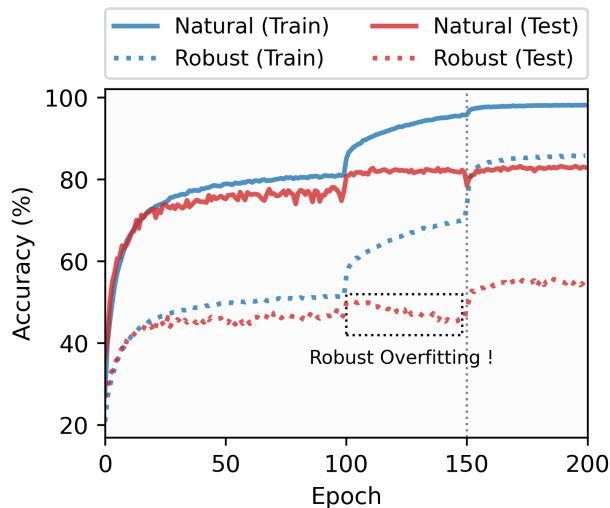


Figure 12. Adversarial training curve of our Elastic DL. During the 100th to 150th epochs, the model experiences a catastrophic *robust overfitting* problem. By introducing the Elastic DL structural prior at the 150th epoch and fine-tuning, we effectively mitigate overfitting and achieve significantly improved robustness and generalization.

Training curves of baseline methods. We track the training curves of the baselines including regularization (ℓ_1 , ℓ_2 regularizations and their combination), Cutout (DeVries, 2017), Mixup (Zhang, 2017) in Figure 13.

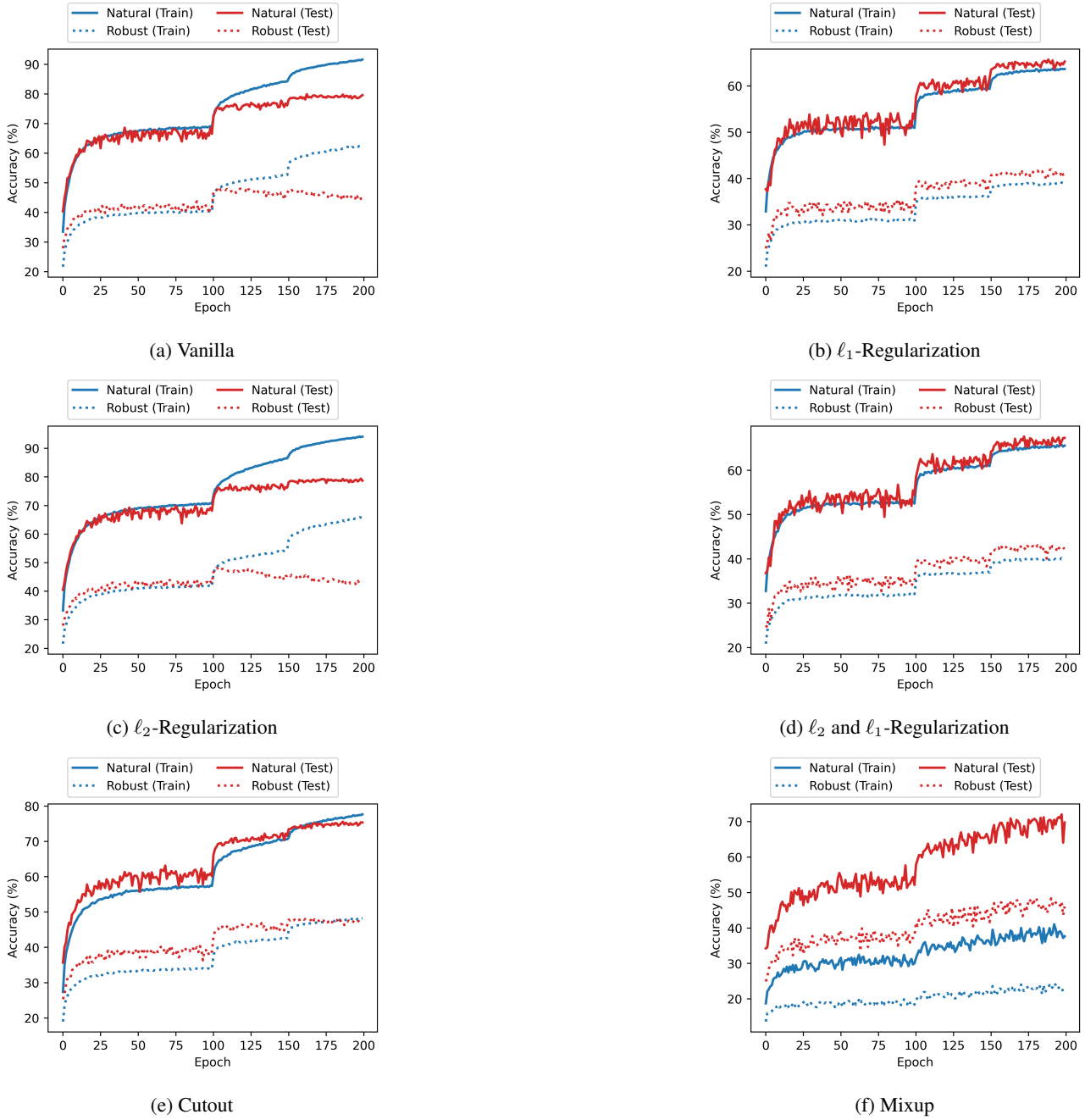


Figure 13. Training curves of baselines.

D.2.2. COMPARISON OF ALL METHODS

To make a comparison of all the methods, we compare the natural and robust performance in the training and testing dataset through the training curve in Figure 14. The figures show the consistent advantage of our Elastic DL over other methods.

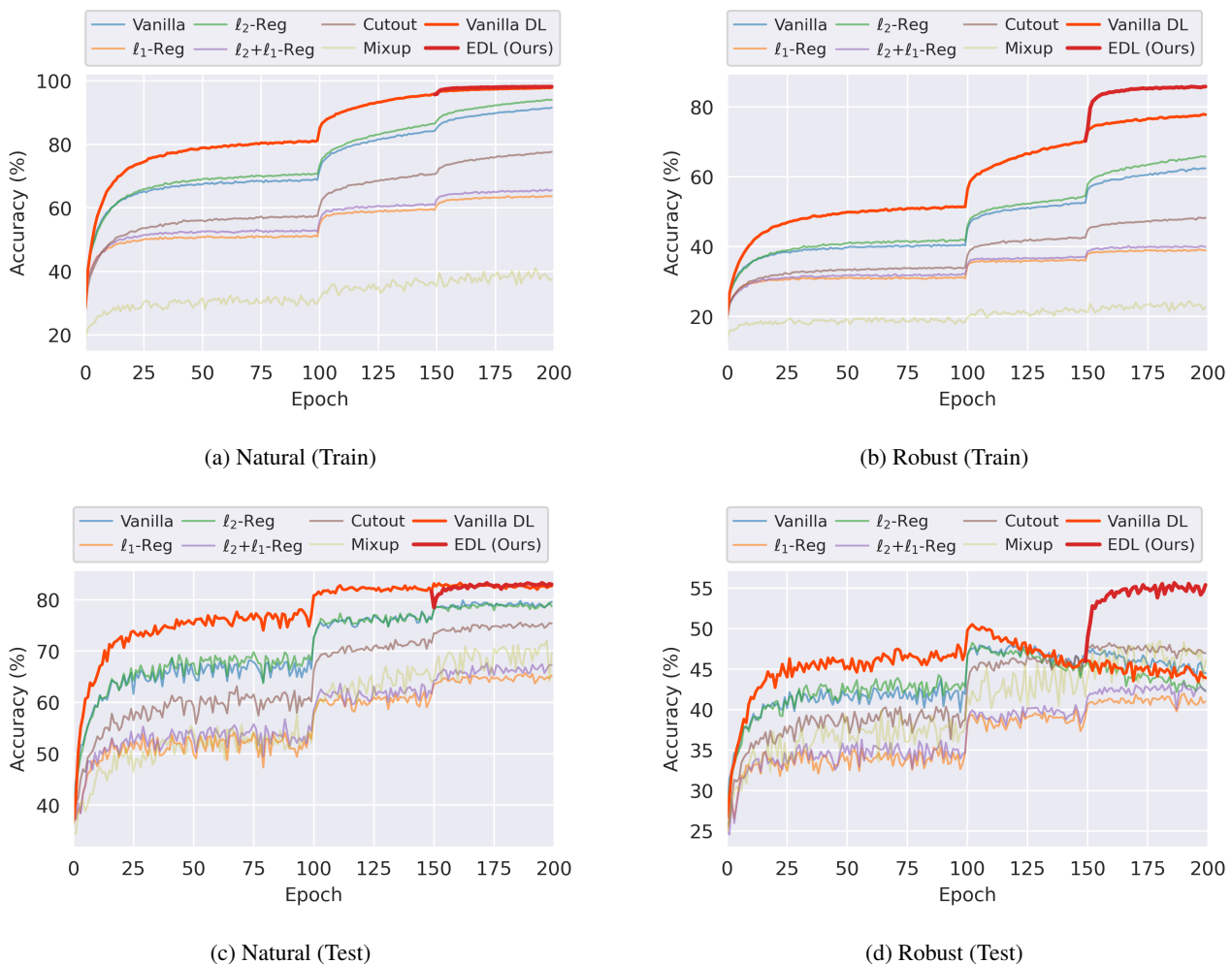


Figure 14. Comparison of training curves of all methods.

D.3. Ablation Studies

D.3.1. UNIVERSALITY

Universality across various backbones, datasets and attacks. We conduct ablation studies on different backbones, datasets, and attacks in Table 8, Table 9, and Table 10. Our proposed method shows consistent effectiveness under various settings.

Table 8. Adversarial robustness on CIFAR10 with different backbones.

METHOD	NATURAL	PGD	FGSM	C&W	AA
VANILLA DL + RESNWT10	81.55	45.48	52.53	45.85	41.60
ELASTIC DL + RESNET10	82.69	49.54	64.52	57.37	46.30
VANILLA DL + RESNWT18	83.28	45.64	53.88	41.22	43.70
ELASTIC DL + RESNET18	83.57	53.22	69.35	60.8	52.90
VANILLA DL + RESNWT34	82.45	45.37	54.32	42.12	44.40
ELASTIC DL + RESNET34	82.95	55.88	70.19	61.74	53.80
VANILLA DL + RESNWT50	81.22	46.83	53.75	43.64	45.10
ELASTIC DL + RESNET50	81.07	58.33	69.38	64.87	56.70

Table 9. Adversarial robustness on CIFAR100 with different backbones.

METHOD	NATURAL	PGD	FGSM	C&W	AA
VANILLA DL + RESNWT10	55.94	22.45	26.57	18.9	21.00
ELASTIC DL + RESNET10	55.20	26.30	35.34	26.45	22.60
VANILLA DL + RESNWT18	57.24	22.17	26.81	17.43	21.60
ELASTIC DL + RESNET18	57.70	27.27	37.62	28.87	26.30
VANILLA DL + RESNWT34	56.18	21.77	26.14	16.38	20.80
ELASTIC DL + RESNET34	56.38	32.67	43.39	39.34	29.20
VANILLA DL + RESNWT50	54.01	22.39	26.4	18.4	20.90
ELASTIC DL + RESNET50	54.64	30.29	41.48	35.24	28.10

Table 10. Adversarial robustness on Tiny-Imagenet with different backbones.

METHOD	NATURAL	PGD	FGSM	C&W	AA
VANILLA DL + RESNWT10	49.6	27.17	32.46	37.91	20.20
ELASTIC DL + RESNET10	50.12	32.93	39.64	40.10	24.90
VANILLA DL + RESNWT18	50.22	31.45	36.46	39.02	30.90
ELASTIC DL + RESNET18	50.52	37.6	43.1	46.64	36.30
VANILLA DL + RESNWT34	50.03	33.54	37.24	37.19	29.30
ELASTIC DL + RESNET34	50.40	34.8	41.75	44.72	34.60
VANILLA DL + RESNWT50	50.35	34.42	37.63	38.86	31.20
ELASTIC DL + RESNET50	50.39	37.38	42.06	41.09	35.40

D.3.2. ORTHOGONALITY TO ADVERSARIAL TRAINING.

Our proposed Elastic DL framework incorporates structural priors into neural networks, complementing existing adversarial training techniques. As shown in Table 4 and Figure 15, Elastic DL can be integrated with various adversarial training methods (PGD-AT, TRADES-2.0/0.2, HAT) to consistently enhance performance.

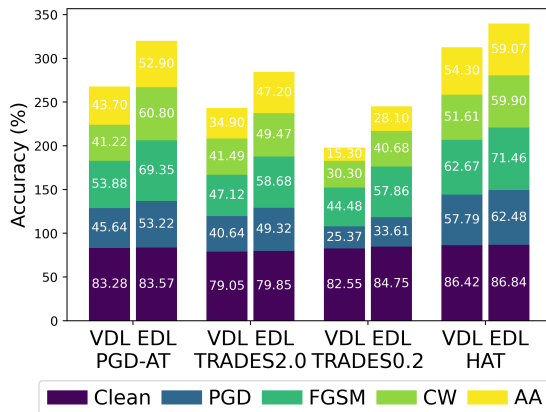


Figure 15. Different adversarial training. Our Elastic DL is orthogonal to existing adversarial training methods and can be combined with them to further improve the performance.

D.3.3. DIFFERENT BUDGET MEASUREMENT

In addition to ℓ_∞ -norm attack (PGD- ℓ_∞), we also validate the consistent effectiveness of our Elastic DL with ℓ_2 -norm (PGD- ℓ_2) and ℓ_1 -norm (SparseFool) attacks in the Figure 16 and Table 11.

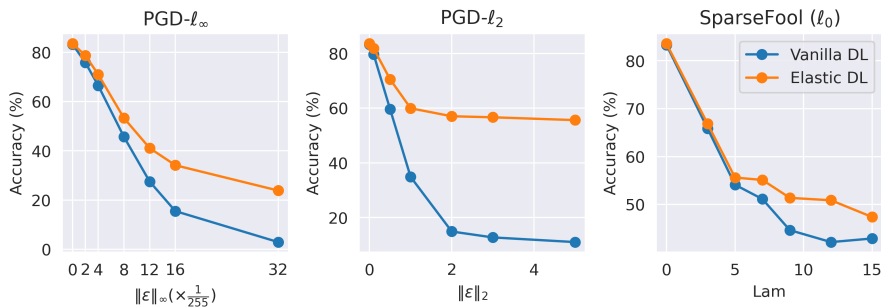


Figure 16. Different attack measurements. Our Elastic DL consistently outperforms Vanilla DL across attacks (PGD- ℓ_∞ , PGD- ℓ_2 , SparseFool) evaluated under various metrics (ℓ_∞ , ℓ_2 , ℓ_0 norms).

Table 11. Adversarial robustness on CIFAR10 with different budget measurements.

PGD $\ \cdot\ _\infty \setminus$ BUDGET	0	2/255	4/255	8/255	12/255	16/255	32/255	
VANILLA DL + RESNWT18	83.29	75.86	66.52	45.66	27.5	15.48	2.89	
PGD-AT+ EDL - RESNET18	83.57	78.76	71.01	53.29	41.1	34.13	23.84	
PGDL2 $\ \cdot\ _2 \setminus$ BUDGET	0	0.1	0.5	1.0	2.0	3.0	5.0	
VANILLA DL + RESNWT18	83.29	79.67	59.64	34.86	14.91	12.75	11.05	
PGD-AT+ EDL - RESNET18	83.57	81.83	70.55	59.95	57.03	56.65	55.62	
SPARSEFOOL $\ \cdot\ _0 \setminus$ LAM	0	3	5	7	9	12	15	20
VANILLA DL + RESNWT18	83.29	65.83	54.11	51.12	44.63	42.14	42.89	41.39
PGD-AT+ EDL - RESNET18	83.57	66.83	55.61	55.11	51.37	50.87	47.38	47.13

D.3.4. HIDDEN EMBEDDING VISUALIZATION

We conduct visualization analyses on the hidden embedding to obtain better insight into the effectiveness of our proposed Elastic DL. We begin by quantifying the relative difference between clean embeddings (x or z_i) and attacked embeddings (x' or z'_i) across all layers. As shown in Figure 17 and Figure 18, the presence of adversarial perturbations can disrupt the hidden embedding patterns, leading to incorrect predictions in the case of Vanilla DL. In contrast, our Elastic DL appears to lessen the effects of such perturbations and maintain predicting groundtruth label.

Here are instances of CAT, SHIP, FROG, AUTOMOBILE, and TRUCK:

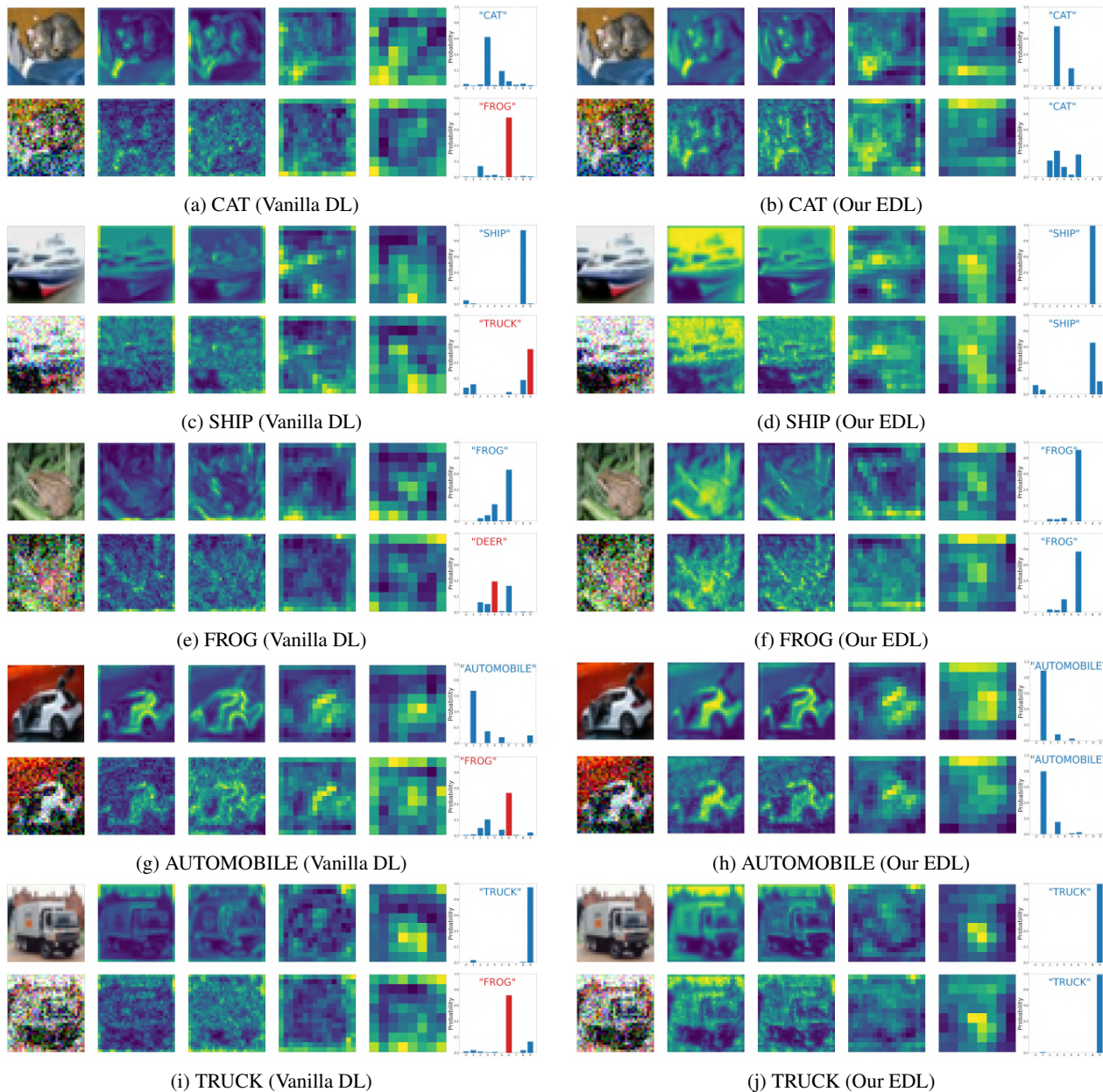


Figure 17. Hidden embedding visualization. (Part 1)

Here are instances of BIRD, HORSE, AIRPLANE, DEER and DOG:

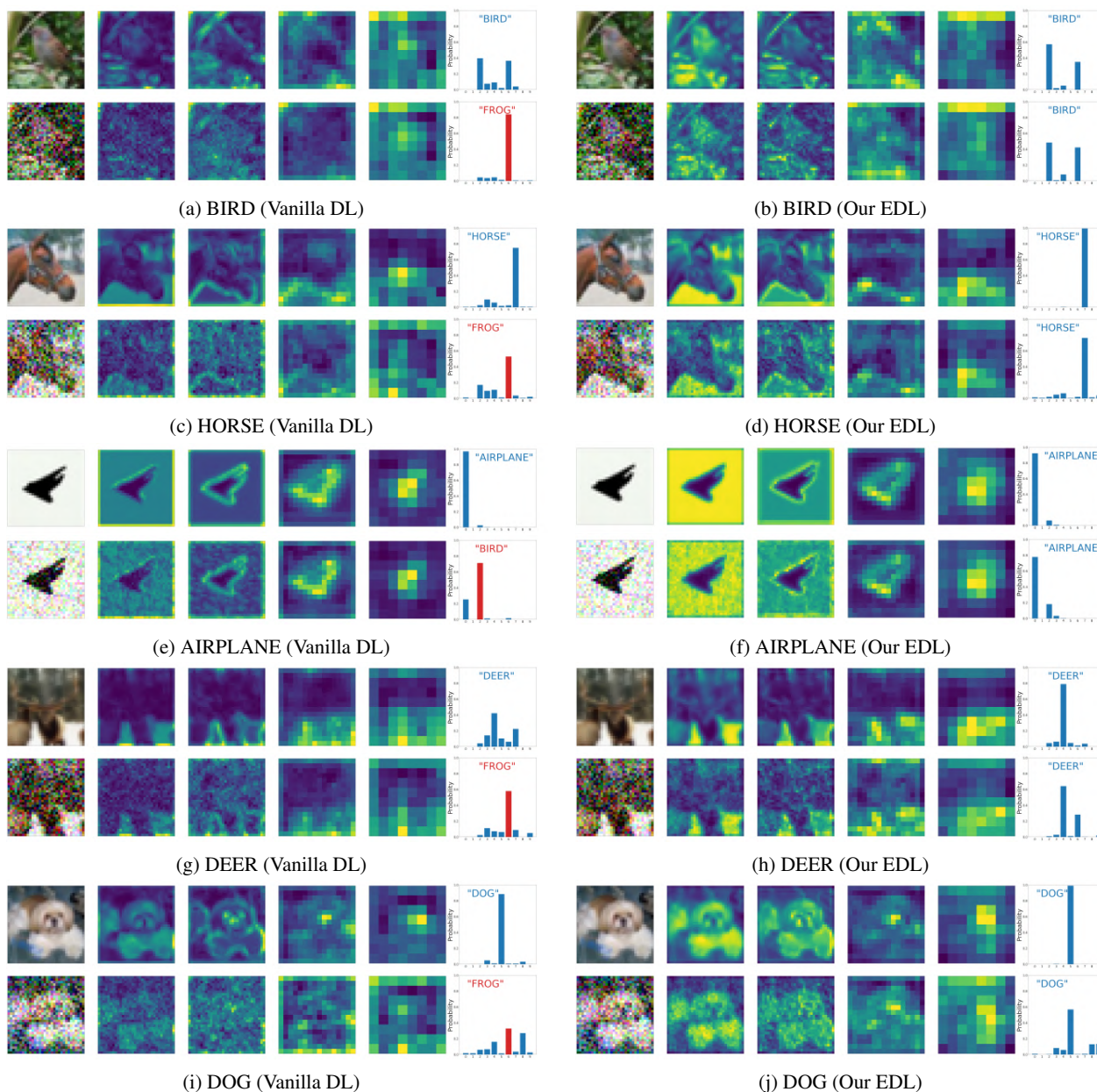


Figure 18. Hidden embedding visualization. (Part 2)

D.3.5. RECONSTRUCTION PROCESS

Image & noise reconstruction. In conventional feedforward neural networks, adding a perturbation ϵ to the input can lead the model to make incorrect predictions. However, as illustrated in Figure 19, our approach aims to reconstruct both the clean image x and the perturbation ϵ through a dictionary learning process. To evaluate the effectiveness of our method, we quantify the reconstruction error between the recovered noise $\hat{\epsilon}$ in our Elastic DL framework and noise generated by various methods (random noise, transfer noise from ResNet/Vanilla DL, and adaptive noise from Elastic DL). As shown in Table 12, the recovered noise from our approach exhibits the smallest difference compared to the adaptive noise in Elastic DL. This result demonstrates that our proposed framework more effectively reconstructs the noise and mitigates its impact on predictions.

Table 12. Reconstruction Error. We quantify the reconstruction error between the recovered noise $\hat{\epsilon}$ and various input noises, including random noise (ϵ_{random}), transfer noise from ResNet (ϵ_{resnet}) and Vanilla DL ($\epsilon_{\text{vanilla}}$), as well as adaptive noise from our Elastic DL ($\epsilon_{\text{elastic}}$). Our Elastic DL demonstrates the smallest reconstruction error, indicating that our approach can adaptively recover and neutralize the input perturbation, thereby mitigating its impact.

ERROR	$\ \cdot\ _1$	$\ \cdot\ _2$	$\ \cdot\ _\infty$
$\epsilon_{\text{RANDOM}} - \hat{\epsilon}$	1294.75 ± 406.78	26.09 ± 7.04	0.901 ± 0.10
$\epsilon_{\text{RESNET}} - \hat{\epsilon}$	131.51 ± 10.53	2.93 ± 0.22	0.163 ± 0.01
$\epsilon_{\text{VANILLA}} - \hat{\epsilon}$	129.07 ± 13.22	2.85 ± 0.26	0.157 ± 0.01
$\epsilon_{\text{ELASTIC}} - \hat{\epsilon}$	122.62 ± 9.92	2.69 ± 0.22	0.149 ± 0.01

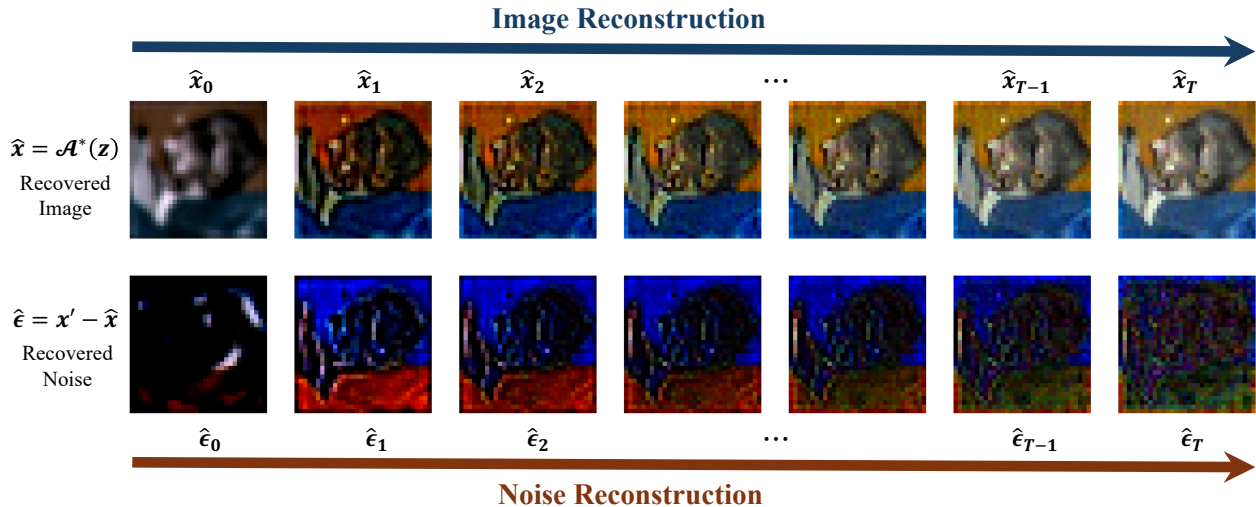


Figure 19. Reconstruction process.